非平衡確率過程による量子化

課題番号 07804017

1995 年度～1997 年度科学研究費補助金 (基盤研究 (C) (2)) 研究成果報告書

1998 年 4 月

研究代表者 中　里　弘　道
(早稲田大学理工学部)

はじめに

本研究課題は，1981年Parisi-Wuにより提唱された確率過程量子化法の枠組みと適用範囲の拡大によって，場の量子化そのものの意味を明らかにしようとねらったものである．特に「仮想時間」に対する確率過程の熱平衡極限を考えるという従来の方法ではなく，熱平衡に至るまでの緩和過程の積極的活用によって，量子化が実行できないか，あるいは物理情報が引き出せないか検討したことが，本研究の独自な点であり特色である．具体的内容としては以下の項目が挙げられる．

1. 非有界の古典的作用Sを持つ統計力学系(自由度1)に対してkernel自由度付き確率過程を設定し，その厳密解及び漸近形を求めた．さらに，この取り扱いを多自由度系へと拡張し，Fokker-Planck方程式の厳密解を見出した．
2. これらの厳密解は，非有界の作用によって記述される仮想的確率過程が熱平衡を持たない拡散過程であることを物語っている．しかし同時に，有限の仮想時間に相当する適当な有限領域で考える限り，経路積分で期待される重み関数e^{-S}が近似的に再現されていることも確認された．
3. kernel自由度付きLangevin方程式に基づく数値シミュレーションで見出されている，いわゆるexcursion phenomenaを理論的に解析した．
4. 非平衡確率過程の臨界現象への適用を試み，平衡状態に達するまでの過渡現象から臨界指数等，物理的に有用な情報が取り出せることを具体例に基づいて示した．
5. この他，確率過程量子化法の応用として，解けるゲージ模型に基づくZwanziger流ゲージ固定項の分析，Coulomb系あるいは境界を持った系に対する遷移確率振幅の導出を試みた．

取り上げた問題の性格上（本研究計画は，当初，一般研究(C)の萌芽的研究として採択された），3ヶ年の研究期間で必ずしも満足できるところまで到達できなかったかもしれない．現時点で取りまとめる成果は，この意味において未だ発展途中である．また，以下で報告する内容の多くは，学術誌に掲載済のものを除くと，早稲田大学大学院博士課程の湯浅一哉氏との共同研究に基づくものである．

最後に，本研究遂行に当たって様々な局面で御支援，御協力いただいた関係諸機関(早稲田大学理工学部及び教務部，徳山大学)及び関係各位に感謝いたします．

1998年4月

研究代表者 中　里　弘　道
（早稲田大学理工学部）

研究組織

研究代表者：中里弘道　（早稲田大学・理工学部・助教授）
研究分担者：金長正彦　（早稲田大学・理工学総合研究センター・講師）
研究分担者：岡野啓介　（徳山大学・経済学部・助教授）

研究経費

1995 年度	500 千円
1996 年度	500 千円
1997 年度	500 千円
計	1,500 千円

研究発表

(1) 学会誌等

- H. Nakazato, M. Namiki, S. Pascazio and H. Rauch, On the quantum Zeno effect, Phys. Lett. A **199** No. 1,2 (1995) 27–32.
- H. Nakazato and S. Pascazio, On the short-time behavior of quantum mechanical systems, Mod. Phys. Lett. A **10** No. 40 (1995) 3103–3111.
- M. Kanenaga and M. Namiki, On the stochastic quantization method: Characteristics and applications to singular systems, in *Proc. of Fourth Int. Conf. on Squeezed States and Uncertainty Relations*, NASA Conference Pub. **3322** (1995) 229–234.
- H. Nakazato, M. Namiki and S. Pascazio, Temporal behavior of quantum mechanical systems, Int. J. Mod. Phys. B **10** No. 3 (1996) 247–295.
- H. Nakazato, M. Namiki, S. Pascazio and H. Rauch, Understanding the quantum Zeno effect, Phys. Lett. A **217** No. 4,5 (1996) 203–208.
- H. Nakazato, M. Namiki, S. Pascazio and Y. Yamanaka, Quantum dephasing by chaos, Phys. Lett. A **222** No. 3 (1996) 130–136.
- K. Machida, H. Nakazato, M. Namiki and S. Pascazio, Effect of fluctuation and dissipation on neutron scattering, J. Phys. Soc. Jpn. **65** Suppl. A (1996) 33–36.

- S. Pascazio, H. Nakazato and M. Namiki, Quantum Zeno effect, J. Phys. Soc. Jpn. **65** Suppl. A (1996) 285–288.
- R. Blasi, H. Nakazato, M. Namiki and S. Pascazio, Dissipative behavior of a quantum system interacting with a macroscopic medium, Phys. Lett. A **223** No. 5 (1996) 320–326.
- O.I. Zavialov, M. Kanenaga, A.I. Kirillov, V.Y. Mamakin, M. Namiki, I. Ohba and E.V. Polyachenko, On quantization of systems with actions unbounded from below, Theor. Math. Phys. **109** No. 2 (1996) 1379–1387.
- R. Blasi, H. Nakazato, M. Namiki and S. Pascazio, Emergence of a Wiener process as a result of the quantum mechanical interaction with a macroscopic medium, Physica A **245** No. 1,2 (1997) 189–211.
- H. Nakazato and S. Pascazio, A solvable model for quantum mechanical dissipation, in *New Perspectives in the Physics of Mesoscopic Systems*, S. De Maritno *et al.* eds., World Sci. Pub. (1997) 216–224.
- H. Nakazato, Time development of a wave packet and the time delay, Found. Phys. **27** No. 12 (1997) 1709–1723.
- K. Okano, L. Schülke, K. Yamagishi and B. Zheng, Universality and scaling in short-time critical dynamics, Nucl. Phys. B **485** No. 3 (1997) 727–746.
- K. Okano, L. Schülke, K. Yamagishi and B. Zheng, Monte Carlo simulation of the short-time behaviour of the dynamic XY-model, J. Phys. A **30** No. 13 (1997) 4527–4535.
- K. Okano, L. Schülke and B. Zheng, Dynamic SU(2) lattice gauge theory at finite temperature, Phys. Rev. D **57** No. 3 (1998) 1411–1414.
- Z. Hradil, H. Nakazato, M. Namiki, S. Pascazio and H. Rauch, Infinitely frequent measurements and quantum Zeno effect, to appear in Phys. Lett. A.
- M. Namiki, H. Nakazato and S. Pascazio, Time symmetry and quantum dephasing, to appear in *Proc. Int. Symp. "Symmetries in Science X"*.
- H. Nakazato, Time development of a wave packet in potential scattering, to appear in *Proc. Int. Symp. "Symmetries in Science X"*.
- S. Pascazio, H. Nakazato and M. Namiki, Temporal behavior of quantum systems and quantum Zeno effect, to appear in *Proc. Int. Symp. "Symmetries in Science X"*.

(2) 口頭発表

- M. Kanenaga and M. Namiki, On the stochastic quantization method: Characteristics and applications to singular systems, *Fourth Int. Conf. on Squeezed States and Uncertainty Relations* (China), 1995.06.05–08.
- 金長正彦・並木美喜雄，確率過程量子化上での不確定性関係の仮想時間発展について，日本物理学会秋の分科会（中部大学），1995.09.27.
- H. Nakazato, K. Machida, M. Namiki and S. Pascazio (Poster presentation), Effect of fluctuation and dissipation on neutron scattering, *Int. Symp. on Advances in Neutron*

Optics and Related Research Facilities (Osaka), 1996.03.20.

- S. Pascazio, H. Nakazato and M. Namiki, Quantum Zeno Effect, *Int. Symp. on Advances in Neutron Optics and Related Research Facilities* (Osaka), 1996.03.21.
- 町田顕・中里弘道・並木美喜雄，観測過程の数値シミュレーション，日本物理学会第51回年会（金沢大学），1996.03.31.
- 中里弘道・堀田浩崇・金長正彦・並木美喜雄，確率過程量子化法にもとづく位相演算子の取り扱い，日本物理学会第51回年会（金沢大学），1996.04.01.
- 町田顕・中里弘道・並木美喜雄，中性子を用いた量子ゼノン効果，日本物理学会秋の分科会（山口大学），1996.10.02.
- 佐々木貴・中里弘道・並木美喜雄，カオス的少数自由度系におけるデフェイジング II，日本物理学会秋の分科会（佐賀大学），1996.10.09.
- 岡野啓介・L Schülke・山岸憲治・B. Zheng，臨界緩和力学の新しいスケーリング則と確率過程量子化，日本物理学会秋の分科会（佐賀大学），1996.10.09.
- 湯浅一哉・中里弘道，確率過程量子化法による遷移確率振幅の計算，日本物理学会秋の分科会（佐賀大学），1996.10.09.
- 町田顕・並木美喜雄・中里弘道・Saverio Pascazio，中性子を用いた量子ゼノン効果 II，日本物理学会第52回年会（名城大学），1997.03.30.
- 荒添直棋・大場一郎・中里弘道，量子力学的コヒーレンスの熱浴との結合による影響，日本物理学会第52回年会（名城大学），1997.03.31.
- 中里弘道，ポテンシャル散乱における波束の時間発展と散乱による波束のずれ，日本物理学会第52回年会（名城大学），1997.03.31.
- 佐々木貴・中里弘道・並木美喜雄，カオス的少数自由度系におけるデフェイジング III，日本物理学会第52回年会（名城大学），1997.03.31.
- 湯浅一哉・中里弘道，確率過程量子化法によるクーロン系の遷移確率振幅の計算，日本物理学会第52回年会（名城大学），1997.03.31.
- M. Namiki, H. Nakazato and S. Pascazio, Time symmetry and quantum dephasing, *International symposium "Symmetries in Science X"* (Bregenz, Austria), 1997.07.15
- H. Nakazato, Time development of a wave packet in potential scattering, *International symposium "Symmetries in Science X"* (Bregenz, Austria), 1997.07.15.
- S. Pascazio, H. Nakazato and M. Namiki, Temporal behavior of quantum systems and quantum Zeno effect, *International symposium "Symmetries in Science X"* (Bregenz, Austria), 1997.07.15.
- 湯浅一哉・中里弘道，確率過程量子化法によるクーロン・ポテンシャルに対する遷移確率振幅の計算，日本物理学会秋の分科会（東京都立大学），1997.09.23.
- 金長正彦・並木美喜雄，ミクロカノニカル量子化に対するカオスの影響，日本物理学会秋の分科会（東京都立大学），1997.09.23.
- R. Blasi・並木美喜雄・中里弘道・S. Pascazio，巨視的媒質との相互作用を取り込んだ力学模型における Wiener 過程の出現機構，日本物理学会秋の分科会（神戸大学），1997.10.05.

- 小山哉・荒添直棋・今福健太郎・町田顕・大場一郎・中里弘道，量子力学的位相相関に及ぼす $1/f$雑音の影響，日本物理学会秋の分科会（神戸大学），1997.10.05.
- 今福健太郎・中里弘道，トンネル現象におけるタイムスケールについて，日本物理学会第53回年会（東邦大学・日本大学），1998.03.31.

（3）出版物

- M. Namiki, S. Pascazio and H. Nakazato, *Decoherence and Quantum Measurements*, (World Scientific Pub., 1998).

§1. 確率過程量子化法と積分核

a. 確率過程量子化法

Parisi-Wu によって提案された確率過程量子化法 [1] では，場 $\phi \equiv \{\phi_i\}$ $(i = 1, \ldots, N)$ の汎関数 $F[\phi]$ の真空期待値 $\langle F[\phi] \rangle$ が，「仮想時間」t に関する Langevin 方程式

$$\frac{\partial}{\partial t}\phi_i(x,t) = -\frac{\delta S[\phi]}{\delta \phi_i(x,t)} + \eta_i(x,t) \tag{1}$$

の解 $\phi_i(x,t)$ から計算される．ここで，$S[\phi]$ は系の Euclid 化された古典作用であり，$\eta_i(x,t)$ は

$$\langle \eta_i(x,t) \rangle = 0, \quad \langle \eta_i(x,t)\eta_j(x',t') \rangle = 2\delta_{ij}\delta^D(x-x')\delta(t-t'), \quad \text{etc.} \tag{2}$$

という統計性を持つ Gauss 型白色雑音である．すなわち，Langevin 方程式 (1) の解を $F[\phi]$ に代入し $\eta_i(x,t)$ についての平均をとって $F[\phi]$ の期待値 $\langle F[\phi(t)] \rangle_\eta$ を計算すれば，量子論的真空期待値はこの熱平衡極限 $t \to \infty$ として再現されるのである：

$$\langle F[\phi] \rangle = \lim_{t\to\infty} \langle F[\phi(t)] \rangle_\eta. \tag{3}$$

このことは，確率変数 $\phi_i(x,t)$ そのものよりも，その背後にある確率分布関数 $P[\phi;t]$ $(\int \mathcal{D}\phi\, P[\phi;t] = 1)$ の時間発展を調べることで明らかになる．分布 $P[\phi;t]$ を，これによって計算される期待値

$$\langle F[\phi] \rangle_t \equiv \int \mathcal{D}\phi\, F[\phi] P[\phi;t] \tag{4}$$

が $\langle F[\phi(t)] \rangle_\eta$ と一致するように導入すると，$\phi_i(x,t)$ は Fokker-Planck 方程式

$$\frac{\partial}{\partial t}P[\phi;t] = H[\phi]P[\phi;t], \tag{5}$$

$$H[\phi] = \int d^D x \frac{\delta}{\delta\phi_i(x)}\left(\frac{\delta}{\delta\phi_i(x)} + \frac{\delta S[\phi]}{\delta\phi_i(x)}\right) \tag{6}$$

に従うことが分かる．Fokker-Planck 演算子 $H[\phi]$ の固有値は 0 以下であるが，最大固有値 0 が離散的で縮退しておらず，さらに $e^{-S[\phi]}$ が規格化可能であるならば，確率分布 $P[\phi;t]$ の熱平衡極限 $P_{\rm eq}[\phi]$ が存在することになる：

$$P_{\rm eq}[\phi] \equiv \lim_{t\to\infty} P[\phi;t] \propto e^{-S[\phi]}. \tag{7}$$

つまり，期待値 (4) の熱平衡極限は

$$\lim_{t\to\infty} \langle F[\phi] \rangle_t = C \int \mathcal{D}\phi\, F[\phi] e^{-S[\phi]} \tag{8}$$

となって，Feynman の経路積分によって計算される真空期待値を再現していることが分かる（C は規格化定数）．

b. 積分核

確率過程量子化では，仮想的な確率過程の熱平衡極限として量子論的真空期待値を与えるわけであるが，同じ熱平衡極限を与える確率過程は一意でなく，無数存在する．実際，系 $S[\phi]$ を量子化するために設定すべき Langevin 方程式は (1) である必要はなく，伊藤型の Langevin 方程式 [2]

$$\frac{\partial}{\partial t}\phi_i(x,t) = \int d^D x' \left(-K_{ij}[\phi;x,x'] \frac{\delta S[\phi]}{\delta \phi_j(x',t)} + \frac{\delta K_{ij}[\phi;x,x']}{\delta \phi_j(x',t)} \right) + \int d^D x'\, G_{ij}[\phi;x,x'] \eta_j(x',t) \tag{9}$$

を用いてもよい．ただし，実汎関数 $K_{ij}[\phi;x,x']$ と $G_{ij}[\phi;x,x']$ との間には

$$K_{ij}[\phi;x,x'] = \int d^D y\, G_{ik}[\phi;x,y] G_{jk}[\phi;x',y] \tag{10}$$

の関係がある．これに対応する Fokker-Planck 演算子は (6) ではなく

$$H[\phi] = \int d^D x\, d^D x' \frac{\delta}{\delta \phi_i(x)} K_{ij}[\phi;x,x'] \left(\frac{\delta}{\delta \phi_j(x')} + \frac{\delta S[\phi]}{\delta \phi_j(x')} \right) \tag{11}$$

となる．正定値の $K_{ij}[\phi;x,x']$ を選べば，$H[\phi]$ の固有値はやはり 0 以下であり，(6) のときと同じ条件下で熱平衡極限が存在して $P_{\rm eq}[\phi] \propto e^{-S[\phi]}$ となるから，期待値の熱平衡極限は真空期待値に等しくなる．$K_{ij}[\phi;x,x']$ は「積分核」(kernel) と呼ばれている．異なる積分核は異なる確率過程に対応するが，正定値性を満たしていればどの積分核を用いても熱平衡極限は同じである．我々は都合のよい（例えば，より早く熱平衡に達するような）積分核を用いて量子化を実行すればよい．

§2. 多自由度底なし系に対する Fokker-Planck 方程式の解析解

a. 積分核を活用した底なし系の確率過程量子化

場の量子論では，重力場などに見られるように，その Euclid 化された作用 S が下に有界でない系がしばしば現れる．このような系は「底なし系」と呼ばれるが，その量子化は困難である．底なし系においては e^{-S} が規格化不可能となるため，e^{-S} は経路積分量子化法での Feynman 測度としても，あるいは確率過程量子化法での熱平衡分布としても採用できず，e^{-S} を重み関数とした通常の意味での真空期待値が定義できないからである．

底なし系の量子化の問題は，より本質的には量子化の意味を改めて問い直す課題とも考えられ，その解決は決して容易でない．これまでにいくつかの野心的な手法が提案されてはいるが，いづれも提案の域を出ていない．このような中で，上述の確率過程量子化法を活用してこの問題に挑戦できないか，というのが本研究の背景でもあった．確率過程量子化法に内在する何らかの自由度を利用しようというのがその基本的アイデアである．このような試みは2つに大別することができよう．ひとつは規格化不可能な e^{-S} はあきらめ，Fokker-Planck

演算子 $H[\phi]$ の規格化可能な固有関数を重み関数として採用 [3] しようというものである．これは，ある意味では極めて大胆な提案であると考えられる．これと対極にあると考えられるのが，以下で述べる方法であり，何らかの意味で e^{-S} を保持し，期待値もこれを重み関数として計算しよう [4] というものである．その基本方程式は積分核を取り入れた Langevin 方程式 (9) である．$S[\phi]$ が底なし系の場合，確率変数 $\phi(x)$ は拡散してしまって熱平衡極限が存在しないわけであるが，積分核をうまく選ぶことで確率変数の拡散を抑制し，有限の仮想時間に相当した有限の領域内で確率分布 e^{-S} を実現する，というのが基本的アイデアである．

例えば，次のような底なし系

$$S[\phi] = S_2[\phi] - S_4[\phi], \tag{12a}$$

$$S_2[\phi] = \int d^D x \left[\frac{1}{2}(\partial_\mu \phi(x))^2 + \frac{1}{2}m^2\phi^2(x)\right], \tag{12b}$$

$$S_4[\phi] = \int d^D x \, \frac{\lambda}{4}\phi^4(x), \qquad \lambda > 0 \tag{12c}$$

の場合には，積分核として

$$K[\phi; x, x'] = e^{-S_4[\phi]}\delta^D(x - x') \tag{13}$$

を用いると，Langevin 方程式 (9) は

$$\frac{\partial}{\partial t}\phi(x,t) = -e^{-S_4[\phi]}\frac{\delta S_2[\phi]}{\delta\phi(x,t)} + e^{-\frac{1}{2}S_4[\phi]}\eta(x,t) \tag{14}$$

となり，確率変数の拡散を抑えるドリフト項を持たせることができる．実際，この Langevin 方程式が（ある意味において）$e^{-S[\phi]}$ を再現することは，0 次元（$D = 0$）での数値シミュレーション [4] により確認されている．こうして得られる e^{-S} を用いて量子化を実行しようというのが基本的アイデアである．

ここで，計算機による Langevin シミュレーションは，結局のところ有限の時間内における有限の領域内に限られた話であることに注意しておく必要がある．底なし系に対して e^{-S} を実現しようというときには，このような事情が念頭にあることを理解しておくべきである．

b. 底なし系に対する Fokker-Planck 方程式の解析解

上述のような底なし系に対する議論は，当初，数値的解析によるところが大きかった．積分核の入った Langevin 方程式 (9), あるいは Fokker-Planck 方程式 (5), (11) を解析的に解くことはまず不可能と考えられたからである．しかし，最近になって，解析的な取り扱いへの可能性が開かれた．任意の 1 自由度底なし系 $S(x)$ に対する Fokker-Planck 方程式

$$\frac{\partial}{\partial t}P(x,t) = \frac{\partial}{\partial x}K(x)\left(\frac{\partial}{\partial x} + S'(x)\right)P(x,t) \tag{15}$$

は，積分核 $K(x)$ を適当に選ぶことで解析的に解ける [5] ということが示されたからである．

実際，Fokker-Planck 演算子の固有値は 0 以下であることがわかっているので

$$P(x,t) = e^{-c^2 t} e^{-S(x)} \tilde{P}(x) \tag{16}$$

とおくと，Fokker-Planck 方程式 (15) は

$$\begin{aligned} -c^2 \tilde{P}(x) &= \left(\frac{d}{dx} - S'(x) \right) K(x) \frac{d}{dx} \tilde{P}(x) \\ &= K(x) \left[\frac{d^2}{dx^2} - \left\{ S'(x) - (\ln K(x))' \right\} \frac{d}{dx} \right] \tilde{P}(x) \end{aligned} \tag{17}$$

となる．ここでさらに，変数変換 $x \to f = f(x)$ を行えば

$$K(x) \left[\left(f'(x) \right)^2 \frac{d^2}{df^2} + \left\{ f''(x) - \left(S'(x) - (\ln K(x))' \right) f'(x) \right\} \frac{d}{df} + c^2 \right] \tilde{P}(x) = 0 \tag{18}$$

となるが，$K(x)$ と $f(x)$ が

$$\begin{cases} K(x) \left(f'(x) \right)^2 = \alpha^2, \\ f''(x) - \left(S'(x) - (\ln K(x))' \right) f'(x) = 0 \end{cases} \tag{19}$$

という条件を満足するならば，$\tilde{P}(x)$ に対する方程式は

$$\left(\alpha^2 \frac{d^2}{dx^2} + c^2 \right) \tilde{P}(x) = 0 \tag{20}$$

となって，解析的に解くことが可能となる．ここで，$\alpha \neq 0$ は実数である．さらに $K(x) = e^{-W(x)}$ とおくと条件 (19) の第 1 式から $f'(x) = \alpha e^{\frac{1}{2} W(x)}$，さらに第 2 式から $W'(x) = -2S'(x)$ を得る．つまり，条件 (19) は

$$\begin{cases} K(x) = e^{2S(x)}, \\ f(x) = \alpha \displaystyle\int_{x_0}^{x} dy\, e^{-S(y)} + \beta \end{cases} \tag{21}$$

によって満足されることが分かる．ここで，β は $x = x_0$ に対応する f の値である（$f(x_0) = \beta$）．

結局，任意の 1 自由度底なし系 $S(x)$ に対しては，積分核 $K(x)$ (21) を採用することで Fokker-Planck 方程式 (15) の解析解が求められるのである．その一般解は，方程式 (20) の解の重ね合わせとして与えられる：

$$P(x,t) = \int_{-\infty}^{\infty} dc\, e^{-c^2 t} e^{-S(x)} \mathrm{Re} \left(A(c) e^{i \frac{c}{\alpha} f(x)} \right). \tag{22}$$

ここで重み関数 $A(c)$ は $P(x,t)$ に課される規格化条件

$$\int_{-\infty}^{\infty} dx\, P(x,t) = 1 \tag{23}$$

と初期条件 $P(x,0)=P_0(x)$ から決められる．規格化条件を (22) に課すと，Jacobian が $f'(x)=\alpha e^{-S(x)}$ であること，底なし系の場合には 1 対 1 で $x\in(-\infty,\infty)\mapsto f\in(-\infty,\infty)$ であることに注意して，(23) は

$$\int_{-\infty}^{\infty}dx\,P(x,t)=\int_{-\infty}^{\infty}\frac{df}{\alpha}\int_{-\infty}^{\infty}dc\,e^{-c^2t}\mathrm{Re}\left(A(c)e^{i\frac{c}{\alpha}f}\right)=2\pi\mathrm{Re}A(0)\equiv 1 \tag{24}$$

となるが，特に初期条件が $P_0(x)=\delta(x-x_0)$ の場合には $A(c)=1/2\pi$ とすればよい．実際この $A(c)$ は (24) を満たしており，確かに初期分布を与えている：

$$P(x,0)=\int_{-\infty}^{\infty}dc\,e^{-S(x)}\mathrm{Re}\left(\frac{1}{2\pi}e^{i\frac{c}{\alpha}f(x)}\right)=e^{-S(x)}\delta\left(\frac{1}{\alpha}f(x)\right)=\delta(x-x_0). \tag{25}$$

結局，初期条件 $P_0(x)=\delta(x-x_0)$ に対する Fokker-Planck 方程式 (15) の解，すなわち Green 関数 $P(x,t;x_0)$ は，

$$\begin{aligned}P(x,t;x_0)&=\int_{-\infty}^{\infty}dc\,e^{-c^2t}e^{-S(x)}\mathrm{Re}\left(\frac{1}{2\pi}e^{i\frac{c}{\alpha}f(x)}\right)\\&=e^{-S(x)}\frac{1}{\sqrt{4\pi t}}\exp\left[-\frac{1}{4t}\left(\int_{x_0}^{x}dy\,e^{-S(y)}\right)^2\right]\end{aligned} \tag{26}$$

と表されることが分かる．また，任意の初期条件 $P_0(x)$ に対する解は

$$P(x,t)=\int_{-\infty}^{\infty}dx'P(x,t;x')P_0(x') \tag{27}$$

として求められる．こうして，適当な積分核を選ぶことによって，任意の 1 自由度底なし系に対する Fokker-Planck 方程式 (15) は解析的に解けることが示されたわけである．

さて，得られた解析解からは，この確率過程が拡散過程であって熱平衡極限の存在しないこと，しかしその一方で，ある意味において $e^{-S(x)}$ が実現されていることを確認することができる．初期条件が $P_0(x)=\delta(x-x_0)$ である場合の解析解は (26) で与えられたが，この初期条件は，Langevin シミュレーションにおいては，初期値 $x(0)=x_0$ から出発して $x(t)$ の時間発展を追って行くことに対応する．今この初期値 x_0 のまわりに $|x-x_0|<R$ という領域 D_R を考え，

$$4t_R=\left(\int_{x_0-R}^{x_0+R}dy\,e^{-S(y)}\right)^2 \tag{28}$$

によって仮想時刻 t_R を導入する．すると時刻 t_R における分布は，D_R 内において近似的に

$$P(x,t_R;x_0)\sim\frac{1}{Z_R}e^{-S(x)},\qquad |x-x_0|<R \tag{29}$$

となっていることが分かる．ただし，Z_R は領域 D_R 内における $e^{-S(x)}$ の規格化定数である：

$$Z_R=\int_{x_0-R}^{x_0+R}dy\,e^{-S(y)}. \tag{30}$$

すなわち，有限の領域 $|x-x_0|<R$ 内で規格化された $e^{-S(x)}$ が，その領域の大きさに応じて決まる有限の仮想時刻 t_R において近似的に実現されているのである．

既に述べたように，このことは，数値シミュレーションにおける $e^{-S(x)}$ の実現とも深い関連がある．計算機上では，無限に広い領域を確保することは原理的に不可能である．必然的にある有限の，しかし十分に大きな領域を設定せざるを得えない．系が下に有界である場合，場の変数は無限遠では十分早く0となるので，このような設定でも数値計算上実質的に困ることはないであろう．しかし，底なし系のように有界でない作用を持った系の場合には，(何もしなければ) 場の変数は無限遠へと拡散してしまうから，有限な領域しか確保できないことは数値計算上実際的困難をもたらす．このような場合には，無限に長い時間ではなく，確保した有限領域に対応した適当な時刻でシミュレーションを打ち切るべきである．重み関数 $e^{-S(x)}$ をこの有限領域（例えば $|x-x_0|<R$）で実現しようとするならば，シミュレーションを行う時間は (28) で与えられる t_R とすればよい，というのが解析解 (26) の教えるところである．

c. 多自由度底なし系に対する Fokker-Planck 方程式の解析解

前節の議論は専ら1自由度系に限られていたが，より現実的な議論をするためには場の理論（無限自由度系）への拡張が望まれる．そこで，ここではその前段階として，多自由度系への拡張を行う．すなわち，積分核 $K_{ij}(x)$ $(i,j=1,\ldots,N)$ を適当に選べば，任意の N 自由度底なし系 $S(x)$ に対する Fokker-Planck 方程式

$$\frac{\partial}{\partial t}P(x,t)=\frac{\partial}{\partial x_i}K_{ij}(x)\left(\frac{\partial}{\partial x_j}+\frac{\partial S(x)}{\partial x_j}\right)P(x,t) \tag{31}$$

は解析的に解けることを示す．さらに，この解析解からは，重み関数 $e^{-S(x)}$ との関係も明らかになる．

まず，1自由度の場合に習って，この Fokker-Planck 方程式が解析的に解けるための積分核に対する条件を見出すことが肝要である．(16) と同様に

$$P(x,t)=e^{-c^2t}e^{-S(x)}\tilde{P}(x) \tag{32}$$

とおくと Fokker-Planck 方程式 (31) は

$$\begin{aligned}-c^2\tilde{P}(x)&=\left(\frac{\partial}{\partial x_i}-\frac{\partial S(x)}{\partial x_i}\right)K_{ij}(x)\frac{\partial}{\partial x_j}\tilde{P}(x)\\&=\left[K_{ij}(x)\frac{\partial^2}{\partial x_i\partial x_j}+\left(\frac{\partial K_{ij}(x)}{\partial x_i}-\frac{\partial S(x)}{\partial x_i}K_{ij}(x)\right)\frac{\partial}{\partial x_j}\right]\tilde{P}(x)\end{aligned} \tag{33}$$

となる．さらに変数変換 $x_i\to f_i=f_i(x)$ を行うと

$$\left[K_{ij}\frac{\partial f_k}{\partial x_i}\frac{\partial f_l}{\partial x_j}\frac{\partial^2}{\partial f_k\partial f_l}+\left\{K_{ij}\frac{\partial^2 f_l}{\partial x_i\partial x_j}+\left(\frac{\partial K_{ij}}{\partial x_i}-\frac{\partial S}{\partial x_i}K_{ij}\right)\frac{\partial f_l}{\partial x_j}\right\}\frac{\partial}{\partial f_l}+c^2\right]\tilde{P}=0. \tag{34}$$

したがって，$K_{ij}(x)$ と $f_l(x)$ が

$$\begin{cases} K_{ij}(x)\dfrac{\partial f_k(x)}{\partial x_i}\dfrac{\partial f_l(x)}{\partial x_j} = h_{kl}, \\ K_{ij}(x)\dfrac{\partial^2 f_l(x)}{\partial x_i \partial x_j} + \left(\dfrac{\partial K_{ij}(x)}{\partial x_i} - \dfrac{\partial S(x)}{\partial x_i}K_{ij}(x)\right)\dfrac{\partial f_l(x)}{\partial x_j} = 0 \end{cases} \tag{35}$$

という条件を満足するならば，$\tilde{P}(x)$ に対する方程式は

$$\left(h_{kl}\frac{\partial^2}{\partial f_k \partial f_l} + c^2\right)\tilde{P}(x) = 0 \tag{36}$$

となり，解析的に解くことが可能となる：

$$\tilde{P}(x) \sim e^{ic_i f_i(x)}, \qquad -h_{ij}c_i c_j + c^2 = 0. \tag{37}$$

ここで，h_{ij} は任意の正実対称定数行列である．

さて，Fokker-Planck 方程式 (31) が解析的に解けるための条件 (35) はさらに簡単にすることができる．(35) の第 2 式は

$$\frac{\partial}{\partial x_i}\left(\frac{\partial f_l}{\partial x_j}K_{ij}e^{-S}\right) = 0 \tag{38}$$

と書き直されるが，(35) の第 1 式を用いて K_{ij} を h_{kl} に置き換え，h_{kl} が定数行列であること，h_{kl} は固有値が正であり逆行列が存在することを考慮すると

$$\frac{\partial}{\partial x_i}\left(\frac{\partial x_i}{\partial f_k}e^{-S}\right) = 0. \tag{39}$$

さらに，公式

$$\frac{\partial}{\partial x_i}\frac{\partial x_i}{\partial f_k} = \frac{\partial}{\partial f_k}\ln\det\left(\frac{\partial x}{\partial f}\right) \tag{40}$$

を用いると (35) の条件は

$$\frac{\partial}{\partial f_k}\ln\det\left(\frac{\partial x}{\partial f}\right) - \frac{\partial S}{\partial f_k} = 0 \tag{41}$$

となり，結局，

$$\det\left(\frac{\partial f(x)}{\partial x}\right) = \alpha e^{-S(x)} \tag{42}$$

という Jacobian に対する条件（$\alpha \neq 0$ は実数）に帰着されることが分かる．Fokker-Planck 方程式 (31) の積分核 $K_{ij}(x)$ は，条件 (42) を満たす変数変換に対して，条件 (35) の第 1 式から決めればよい．

条件 (42) を満たす変数変換としては，例えば次のようなものが考えられる：

$$\begin{cases} f_i(x) = x_i \qquad (i = 1, \ldots, N-1), \\ f_N(x) = \int^{x_N} dy\, e^{-S(x_1, \ldots, x_{N-1}, y)}. \end{cases} \tag{43}$$

実際，この場合

$$\left(\frac{\partial f}{\partial x}\right) = \begin{pmatrix} 1 & 0 & \ldots & 0 \\ & \ddots & \ddots & \vdots \\ & & 1 & 0 \\ * & \ldots & * & e^{-S} \end{pmatrix} \tag{44}$$

となって，(42) を満たしていることが分かる．

さて，Fokker-Planck 方程式 (31) の一般解は (37) の重ね合わせで与えられる：

$$P(x,t) = \int d^N c\, e^{-h_{ij} c_i c_j t} e^{-S(x)} \mathrm{Re}\left(A(c) e^{i c_i f_i(x)}\right). \tag{45}$$

これに規格化条件

$$\int d^N x\, P(x,t) = 1 \tag{46}$$

を課すと，Jacobian が $\det(\partial f(x)/\partial x) = \alpha e^{-S(x)}$ であることに注意して

$$\int d^N x\, P(x,t) = \int \frac{d^N f}{\alpha} \int d^N c\, e^{-h_{ij} c_i c_j t} \mathrm{Re}\left(A(c) e^{i c_i f_i}\right) = \frac{1}{\alpha}(2\pi)^N \mathrm{Re} A(0) \equiv 1 \tag{47}$$

となる．特に初期条件が $P_0(x) = \delta^N(x - x_0)$ の場合には $A(c) = \alpha/(2\pi)^N$ とすればよい：

$$P(x,0) = \int d^N c\, e^{-S(x)} \mathrm{Re}\left[\frac{\alpha}{(2\pi)^N} e^{i c_i f_i(x)}\right] = \alpha e^{-S(x)} \delta^N(f(x)) = \delta(x - x_0). \tag{48}$$

ただし，$f(x_0) = 0$．結局，Green 関数 $P(x,t;x_0)$ は

$$\begin{aligned} P(x,t;x_0) &= \int d^N c\, e^{-h_{ij} c_i c_j t} e^{-S(x)} \mathrm{Re}\left[\frac{\alpha}{(2\pi)^N} e^{i c_i f_i(x)}\right] \\ &= \alpha e^{-S(x)} \frac{1}{\sqrt{(4\pi t)^N \det(h_{ij})}} \exp\left(-\frac{1}{4t} h^{-1}_{ij} f_i(x) f_j(x)\right) \end{aligned} \tag{49}$$

となる．したがって，任意の初期条件 $P_0(x)$ に対する解は

$$P(x,t) = \int d^N x'\, P(x,t;x') P_0(x') \tag{50}$$

と表される．

さて，この解析解と $e^{-S(x)}$ の関係を調べてみよう．仮想時刻 t_R を，例えば，x_0 を囲む有限領域

$$D_R : h^{-1}_{ij} f_i(x) f_j(x) < 4 t_R \Gamma^{\frac{2}{N}} \left(\frac{N}{2} + 1\right) \equiv a_R^2 \tag{51}$$

によって導入すると，この領域内における $e^{-S(x)}$ の規格化定数は

$$Z_R \equiv \int_{D_R} d^N x\, e^{-S(x)} = \int_{D_R} \frac{d^N f}{\alpha} = \frac{1}{\alpha}\sqrt{(4\pi t_R)^N \det(h_{ij})} \tag{52}$$

となる．最後の等号は，領域 D_R が h_{ij}^{-1} を対角化する変換 $f_i \to y_i$ によって $\lambda_1^{-1}y_1^2 + \cdots + \lambda_N^{-1}y_N^2 < a_R^2$（$\lambda_i$ は h_{ij} の固有値）に，さらに変換 $y_i = \lambda_i^{1/2} z_i$ で $z_1^2 + \cdots + z_N^2 < a_R^2$ となることから，半径 a_R の N 次元球の体積 $\sqrt{(\pi a_R^2)^N \Gamma^{-1}(N/2+1)} = \sqrt{(4\pi t_R)^N}$ に変換の Jacobian $\sqrt{\det(h_{ij})}$ を乗じて得られる．$\Gamma^{2/N}(N/2+1) = O(1)$*であるならば，その領域内で，確率分布関数は

$$P(x, t_R; x_0) \sim \frac{1}{Z_R} e^{-S(x)}, \qquad x \in D_R \tag{53}$$

と近似することができる．

こうして，任意の N 自由度底なし系に対する Fokker-Planck 方程式 (31) は適当な積分核の導入で解析的に解けることが示された．また，$e^{-S(x)}$ との関連も明らかにすることができた．

解析的に解けるための条件は (35) 第1式と Jacobian に対する条件 (42) であった．この条件を満たす変数変換を構成することは実際に可能であり，ここでは一例として (43) を挙げた．ただ，この先さらに場の理論（無限自由度系）へと拡張する上で，この変換は適当でない．連続極限 $x_i \to x(s)$ が取れないからである．場の理論へ適用するためには，別の変数変換を見出すことが必要であり，今後の課題のひとつである．

最後に，このような拡散過程を利用する際の注意として，その初期値あるいは初期分布依存性を考えておく必要がある．この点に関しては，これまでのところ詳しい検討がなされた訳ではないが，上の議論から分かることは，確率変数が拡散型の確率微分方程式に従ってある有限領域内に拡散し，この領域内で $e^{-S(x)}$ を近似的に実現しているような時刻 t_R は，確かに初期値 x_0 としてどんな値を取るか，つまり，底なしポテンシャルのどのあたりから出発するのかに大きく依存することが予想される．その一方で，領域の大きさと t_R が適切に選ばれていれば，そこで実現される分布は，$e^{-S(x)}$ を（基本的には初期値 x_0 とは関係なく）十分よく近似することができるだろう．いずれにしても，さらに詳しい分析が必要である．

References

[1] G. Parisi and Y.-S. Wu, Sci. Sin. **24** (1981) 483.
確率過程量子化法に関しては次の総合報告も参考になる．
P. H. Damgaard and H. Hüffel, Phys. Rep. **152** (1987) 227;
M. Namiki, *Stochastic Quantization*, (Springer-Verlag, 1992).

[2] 例えば，
C. G. Gardiner, *Handbook of Stochastic Methods for Physics, Chemistry and the Natural Sciences*, (Springer-Verlag, New York, 1985).

* $N \to \infty$ で $\Gamma^{2/N}(N/2+1) \sim (N/2)e^{-1}$ である．

[3] J. Greensite and M. B. Halpern, Nucl. Phys. **B242** (1984) 167;
J. Greensite, Nucl. Phys. **B361** (1991) 729;
J. Greensite, *ibid.* **B439** (1993) 439.

[4] S. Tanaka, M. Namiki, I. Ohba, M. Mizutani, N. Komoike and M. Kanenaga, Phys. Lett. **B288** (1992) 129;
S. Tanaka, I. Ohba, M. Namiki, M. Mizutani, N. Komoike and M. Kanenaga, Prog. Theor. Phys. **89** (1993) 187;
M. Kanenaga, M. Mizutani, M. Namiki, I. Ohba and S. Tanaka, Prog. Theor. Phys. **91** (1994) 599.

[5] H. Nakazato, Phys. Lett. **B333** (1994) 98.

Theoretical and Mathematical Physics, Vol. 109, No. 2, 1996

ON QUANTIZATION OF SYSTEMS WITH ACTIONS UNBOUNDED FROM BELOW

O. I. Zavialov,[1] M. Kanenaga,[2] A. I. Kirillov,[1] V. Yu. Mamakin,[1] M. Namiki,[2] I. Ohba,[2] and E. V. Polyachenko[1]

We consider two possible approaches to the problem of the quantization of systems with actions unbounded from below: the Borel summation method applied to the perturbation expansion in the coupling constant and the method based on the kerneled Langevin equation for stochastic quantization. In the simplest case of an anharmonic oscillator, the first method produces Schwinger functions, even though the corresponding path integral diverges. The solutions of the kerneled Langevin equation are studied both analytically and numerically. The fictitious time averages are shown to have limits that can be considered as the Schwinger functions. The examples demonstrate that both methods may give the same result.

1. Introduction

Let $G_1(x)$, $G_2(x_1, x_2)$, ..., $G_n(x_1, \ldots, x_n)$, ... be the Schwinger functions of some quantum field. In practice, they are defined by the path integrals as follows:

$$G_n(x_1, \ldots, x_n) = \mathcal{N} \int \varphi(x_1) \ldots \varphi(x_n)\, e^{-A[\varphi]}\, \mathcal{D}\varphi, \tag{1}$$

where $\mathcal{N}$ is the normalizing factor and $A[\cdot]$ is the Euclidean action functional.

For example, for the scalar field φ,

$$A[\varphi] = \frac{1}{2} \int \left[(\partial_\mu \varphi)^2 + m^2 \varphi^2\right] d^d x + \frac{\lambda}{4} \int \varphi^4\, d^d x. \tag{2}$$

Among the various mathematical problems involved in path integral calculation (2), there is a special problem that appears when λ is negative. There, action $A[\cdot]$ is not bounded from below and, obviously, the path integral (1) diverges. Systems with such action functionals are called *bottomless*.

In classical mechanics, there are many models where the energy is unbounded from below which also possess regular dynamic behavior. The quantum Heisenberg description of the related models also has no principal drawbacks. Thus, one can infer that Schwinger functions might exist (in some sense) for systems with actions unbounded from below. In this paper, we discuss the two following approaches to bottomless systems:

1. Analytic continuation in λ;
2. Stochastic quantization.

The perturbation expansion in λ for G_n is well defined in every order, irrespective of the sign of the coupling constant. As the perturbation series is apparently divergent, we apply the Borel method to sum the asymptotic expansions.

The simplest stochastic quantization scheme is not applicable in our case because the solutions of the corresponding Langevin equation blow up, i.e., go to infinity during some finite time period. Therefore, we

[1]Higher College for Mathematical Physics, Moscow Independent University, Moscow.
[2]Physics Department, Waseda University, Tokyo.

Translated from Teoreticheskaya i Matematicheskaya Fizika, Vol. 109, No. 2, pp. 175–186, November, 1996. Original article submitted June 13, 1996.

0040-5779/96/1092-1379$15.00

use the kerneled Langevin equation instead. In this paper, we restrict ourselves to a toy model, considering the $N = 1$ matrix model in $D = 0$ configuration space and we employ both of the above methods to calculate the Schwinger functions. Then the path integral (1) is reduced to an ordinal integral of the form

$$G_n = \mathcal{N} \int_{-\infty}^{\infty} \varphi^n \exp\left(-\frac{\varphi^2}{2} - \lambda\frac{\varphi^4}{4}\right) d\varphi. \tag{3}$$

The paper is organized as follows. In Secs. 2 and 3, we discuss the methods of Borel summation and stochastic quantization. Next, we present the results of computer simulations (Sec. 4) and, finally, (Sec. 5) the concluding remarks.

2. Borel summation method

The idea of applying the Borel summation method to divergent series of perturbation theory first appeared in [1], where an anharmonic oscillator was studied. Later, it turned out that some asymptotic expansions in the $P(\varphi)_2$-theory in infinite volumes are Borel-summable [2]. Borel summability for the Zeemann effect was proved in [3]. Here we revisit this subject for the bottomless case.

Let us consider a power series in λ, formally defined by the integral

$$S_{2k}(\lambda) = \int_{-\infty}^{\infty} \varphi^{2k} \exp\left(-\frac{\varphi^2}{2} - \lambda\frac{\varphi^4}{4}\right) d\varphi.$$

It is easy to check that

$$S_{2k}(\lambda) \sim \sum_{n=0}^{\infty} (-1)^n a_n(k) \lambda^n, \tag{4}$$

where

$$a_n(k) = \sqrt{2\pi}\frac{1}{n!}\frac{(4n+2k-1)!!}{2^{2n}}.$$

Following Borel, one defines an auxiliary function as

$$h_k(u) = \sum_{n=0}^{\infty} \frac{a_n(k)}{n!} u^n. \tag{5}$$

Then the sum of the asymptotic expansion is

$$S_{2k}(\lambda) = \int_0^{\infty} e^{-v} h_k(-\lambda v)\, dv. \tag{6}$$

This expansion of function $h_k(u)$ converges inside the circle $|u| < \frac{1}{4}$. We need to know, however, the function $h_k(u)$ for all real $u > 0$ when $\lambda < 0$, and for all $u < 0$ when $\lambda > 0$, in order to calculate S_{2k} by (6). This means that we are to continue this function analytically outside the circle of convergence.

Inside the circle $|u| < \frac{1}{4}$, power series (4) converges to

$$h_k(u) = \sqrt{2\pi}(2k-1)!! F\left(\frac{2k+1}{4}, \frac{2k+3}{4}; 1; 4u\right), \tag{7}$$

where $F(\alpha, \beta; \gamma; z)$ is the Gaussian hypergeometric function (see Sec. 2.1.1 of [4]). This function is analytical in z in the complex plane with the cut $\mathrm{Re}\, z > 1$, $\mathrm{Im}\, z = 0$.

To obtain $S_{2k}(\lambda)$, one has to calculate the integral

$$S_{2k}(\lambda) = \sqrt{2\pi}(2k-1)!! \int_0^{\infty} e^{-v} F\left(\frac{2k+1}{4}, \frac{2k+3}{4}; 1; -4\lambda v\right) dv. \tag{8}$$

When $\lambda > 0$, this formula is well defined. But, in the bottomless case $\lambda < 0$, principal problems arise because, then, $-4\lambda v$ falls on the cut of the function F. Therefore, we have to choose which of the boundary values we should use while integrating in (8). It is also possible to use a linear combination of the integrals over different sides of the cut for the Schwinger functions $S_{2k}(\lambda)$.

In this oversimplified model, the analytical continuation in λ could be done without using the Borel summation method. In particular,

$$S_{2k}(\lambda) = \sqrt{2}\pi(2k-1)!! \left(\frac{1}{4\lambda}\right)^{2-\frac{2k+1}{4}} \left\{ \frac{1}{\Gamma\left(\frac{2k+1}{4}\right)} \Phi\left(\frac{2k+1}{4}, \frac{1}{2}; \frac{1}{4\lambda}\right) - \right.$$
$$\left. - \frac{2}{\Gamma\left(\frac{2k+1}{4}\right)} \left(\frac{1}{4\lambda}\right)^{\frac{1}{2}} \Phi\left(\frac{2k+3}{4}, \frac{3}{2}; \frac{1}{4\lambda}\right) \right\}. \tag{9}$$

In this formula, $\Phi(a, c; z)$ is the degenerate hypergeometric function, which is integer in arguments z and a of Sec. 6.7.1 of [4]. One may use (9) to define the functions $S_{2k}(\lambda)$ in the domain $\lambda < 0$. Unfortunately, these functions have four branches due to the factors $\lambda^{(2k+1)/4}$ and $\lambda^{-1/2}$. Since each $S_{2k}(\lambda)$ has a nonvanishing imaginary part on either side of the cut, *one is forced to consider linear combinations.* Thus, we conclude that one needs some guiding principle to remove the ambiguities and to make the coefficients uniquely determined.

3. Stochastic quantization

In the stochastic quantization scheme, the Schwinger functions are defined as the equilibrium limits of the expectation values

$$G_n(x_1, \ldots, x_n) = \lim_{t\to\infty} \mathrm{E}\varphi_t(x_1)\varphi_t(x_2)\ldots\varphi_t(x_n), \tag{10}$$

where t is the so-called "fictitious" or "computer" time, E denotes the mathematical expectation, and $\varphi_t(x)$ is a solution to the stochastic Langevin equation

$$d\varphi_t(x) = -\frac{\delta A[\varphi_t]}{\delta\varphi_t(x)}\, dt + \sqrt{2}\, dw_t(x). \tag{11}$$

Here w_t is the standard Wiener process in the configuration space of the quantized system.

In our case, the Langevin equation (11) can be written in the following form:

$$d\varphi_t = -\left(\varphi_t + \lambda\varphi_t^3\right) dt + \sqrt{2}\, dw_t. \tag{12}$$

When $\lambda < 0$, there is a nonzero probability that a solution of Eq. (12) goes to infinity during some finite time period. To make sure, let us find the lifetime T of a solution φ_t.

Denote $\tau^{s,x}$ as the time at which a solution of Eq. (12), satisfying the condition $\varphi_s = x$, leaves any bounded region. This $\tau^{s,x}$ is a random value and it is also possible that $\tau^{s,x} = \infty$. It is obvious that $\tau^{s,x}$ is the lifetime T. If there exists a positive bounded smooth function $V(s, x)$ such that for some $c > 0$,

$$\left\{\frac{\partial}{\partial s} + \frac{\partial^2}{\partial x^2} - (x + \lambda x^3)\frac{\partial}{\partial x}\right\} V \geq cV \tag{13}$$

is valid, then by Theorem 3.4.2 of [5], the following estimate for $\tau^{s,x}$ holds:

$$\mathrm{Prob}\left\{\tau^{s,x} - s < \frac{1}{c}\log\frac{\sup V}{V(s,x)} + \varepsilon\right\} > 0, \tag{14}$$

where ε is any positive number.

Let $V(s,x) = \exp\left[-p(x^2+1)^{-1}\right]$, where p is some positive number. Then (13) is equivalent to

$$(-\lambda-\gamma)x^8 + (-2\lambda-1-4\gamma)x^6 + (-\lambda-5-6\gamma)x^4 - (3+4\gamma)x^2 + (1-\gamma) + 2px^2 > 0,$$

where $\gamma = c/(2p)$. Thus, inequality (13) holds if $\gamma < \min\{-\lambda, 1\}$ and p is a sufficiently large positive number. Doing this from (14), one obtains that

$$\text{Prob}\left\{T < -\frac{1}{2\gamma}\,(\varphi_s^2+1)^{-1} + s + \varepsilon\right\} > 0.$$

In other words, for any initial conditions, the sample paths of some of the solutions to Eq. (12) go to infinity during some finite time period. Circumstantially, this can be seen from the behavior of the moments $\mathrm{E}\varphi_t^n$. By Ito's formula,

$$\mathrm{E}\,\frac{d\varphi_t^n}{dt} = n\,\mathrm{E}\,\varphi_t^{n-2}\left(-\lambda\varphi_t^4 - \varphi_t^2 + n - 1\right).$$

Therefore, for all n such that $(n+1)^2 < -4\lambda n^2(n-1)$, inequality $d\mathrm{E}\varphi_t^n/dt \geq \mathrm{E}\varphi_t^n$ holds, i.e., $\mathrm{E}\varphi_t^n \geq e^t\mathrm{E}\varphi_0^n$. This inequality proves that limits of type (10) do not exist.

Thus, the standard procedure of stochastic quantization cannot be applied in our case.

To calculate the Schwinger functions, we need solutions φ_t that are well defined for all $t > 0$. To overcome this problem, the author of [6] proposed the so-called *kerneled Langevin equation* [7], which has the form

$$d\varphi_t(x) = \int d^dx'\left\{\left[-K(x,x';\varphi_t)\frac{\delta A[\varphi_t]}{\delta\varphi_t(x')} + \frac{\delta K(x,x';\varphi_t)}{\delta\varphi_t(x')}\right]dt + \sqrt{2}K^{1/2}(x,x';\varphi_t)\,dw_t(x')\right\}. \tag{15}$$

Following [8], we denote

$$K(x,x';\varphi) = \delta(x-x')\,\exp[\lambda\varphi^4/4].$$

Then (15) takes the form we use below instead of (12):

$$d\varphi_t = -\varphi_t\exp[\lambda\varphi_t^4/4]\,dt + \sqrt{2}\exp[\lambda\varphi_t^4/8]\,dw_t. \tag{16}$$

By Theorem 3.4.1 of [5], solutions of this equation have infinite lifetimes both for $\lambda \geq 0$ and $\lambda < 0$. Moreover, the solutions are *recurrent*, i.e., they visit every interval of the real axis infinitely many times. This allows us to define the time $T_{a,b}(\tau)$ that the process spends in $[a,b]$ from $t=0$ up to $t=\tau$. Obviously, $T_{a,b}(\tau) < \tau$ and $T_{-\infty,+\infty}(\tau) = \tau$. It follows from (16) that the limit below exists:

$$\lim_{\tau\to\infty}\frac{T_{a,b}(\tau)}{T_{c,d}(\tau)} = \frac{\int_a^b \exp\left(-\frac{\lambda}{4}\varphi^4 - \frac{1}{2}\varphi^2\right)d\varphi}{\int_c^d \exp\left(-\frac{\lambda}{4}\varphi^4 - \frac{1}{2}\varphi^2\right)d\varphi}. \tag{17}$$

This property maintains the connection of the kerneled Langevin equation to our problem. Unfortunately, though relation (17) indicates the existence of a stationary distribution of φ_t as $t\to\infty$, this distribution proves to be non-normalizable in the case $\lambda < 0$.

The principal distinction between the $\lambda \geq 0$ and $\lambda < 0$ cases can be seen if one considers the mean time $T_{a,b}(\tau)/\tau$ in the limit when τ goes to ∞. If $\lambda \geq 0$, then

$$\lim_{\tau\to\infty}\frac{T_{a,b}(\tau)}{\tau} = \frac{\int_a^b \exp\left(-\frac{\lambda}{4}\varphi^4 - \frac{1}{2}\varphi^2\right)d\varphi}{\int_{-\infty}^{\infty} \exp\left(-\frac{\lambda}{4}\varphi^4 - \frac{1}{2}\varphi^2\right)d\varphi} > 0.$$

When $\lambda < 0$,

$$\lim_{\tau\to\infty}\frac{T_{a.b}(\tau)}{\tau} = 0. \tag{18}$$

Due to this distinction, the solutions in the case $\lambda \geq 0$ are called *"non-null,"* whereas if (18) holds the solutions are called *"null."* The "null" solutions are known to have some specific ergodic properties that we discuss below.

Denote by μ the stationary distribution of φ_t that is established when $t \to \infty$. Since it is not a stationary distribution, μ-integrable functions rapidly decrease, roughly speaking. On the other hand, by Eq. (16), the process φ_t spends too much time far from the origin because the dumping action of the drift term $-\varphi_t \exp(\lambda\varphi_t^4/4)$ in (16) is small for large $|\varphi_t|$ (recall that $\lambda < 0$). Therefore, if function f is μ-integrable, then, with considerable probability, $f(\varphi_t) = 0$. More precisely [5],

$$\lim_{T\to\infty} \frac{1}{T} \int_0^T f(\varphi_t)\, dt = 0 \quad \text{almost definitely.} \tag{19}$$

This shows that if $\lambda < 0$, the ergodic equality

$$\int f(\varphi)\, d\mu(\varphi) = \lim_{T\to\infty} \frac{1}{T} \int_0^T f(\varphi_t)\, dt$$

between the expectation value and the time average becomes invalid. For some functions, the expectation value may not exist while the time average may. Hence, one can generalize the method of stochastic quantization using the *time averages* instead of the *expectation values*. In this way, the Schwinger functions should be calculated as

$$G_n(x_1, x_2, \ldots, x_n) = \lim_{T\to\infty} \frac{1}{T} \int_0^T \mathrm{E}\, \varphi_t(x_1)\varphi_t(x_2)\ldots\varphi_t(x_n)\, dt,$$

rather than as in (10). Obviously, this formula is equivalent to (10) in the ergodic case.

In studying the time averages, one should pay attention to the φ_t visits to far-off regions. Such visits are called *excursions above the high level*. Such excursions may happen only after the time interval $[\tau, \tau']$ such that

$$\left| \int_\tau^{\tau'} e^{\lambda\varphi_t^4/8}\, dw_t \right| \gg 1. \tag{20}$$

The probability of the appearance of such time intervals is low when $\lambda < 0$ and high when $\lambda \geq 0$.

Since the drift term in the bottomless case is small when $|\varphi_t| \gg 1$, the process φ_t may return from an excursion only after another time interval $[\tau, \tau']$ when condition (20) is satisfied. However, the probability of the appearance of such a time interval is low. Therefore, one should expect long excursions when $\lambda < 0$. It follows from (16) that if $|\varphi_t| \gg 1$, then $d\varphi_t/dt \approx 0$, provided $|\eta_t|$ is not large. Thus, $\varphi_t \approx$ const during each excursion.

Oppositely, if $\lambda \geq 0$, the probability of fulfilling condition (20) is much greater than if $\lambda < 0$. Therefore, the excursions are frequent and short. The mathematical expectation of the recurrence time is finite when $\lambda \geq 0$ and infinite when $\lambda < 0$ [5].

In the bottomless case $\lambda < 0$, we fix some level L (a positive number) and denote by s_k, e_k the random times when the kth excursion above L begins and ends. Then the contribution of the excursions to the time averages can be separated as follows:

$$\lim_{T\to\infty} \frac{1}{T} \int_0^T f(\varphi_t)\, dt = \lim_{k\to\infty} \frac{1}{e_k} \int_0^{T_k} f(\psi_t)\, dt + \lim_{k\to\infty} \frac{1}{e_k} \sum_{j=1}^{k} f(a_j)(e_j - s_j), \tag{21}$$

where ψ_t is the process confined to the region $[-L, L]$ by reflections at the points $-L$ and L, $T_k = e_k - \sum_{j=1}^{k}(e_j - s_j)$ is the time when $|\varphi_t| < L$ during the period $[0, e_k]$, and each a_j is a random number equal to the value φ_t takes during excursion number j. The first limit on the right-hand side of (21) exists because of the good ergodic properties of the ψ_t process. The existence of the second limit and, hence, the existence of the time average (21), depend on the stochastic properties of the random numbers a_j, s_j, and e_j. The fact that the excursions are few and far between hinders its observation in computer simulations and, therefore, one runs the risk of obtaining a wrong value for the time average because of an inaccurate evaluation of the excursion term on the right-hand side of (21).

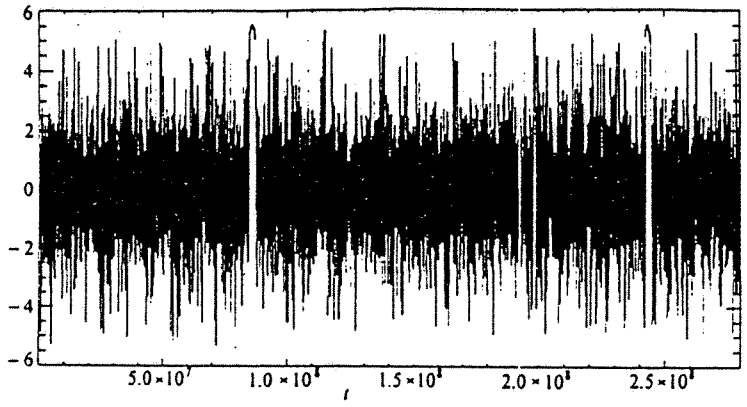

Fig. 1. Typical sample path of the φ_t process.

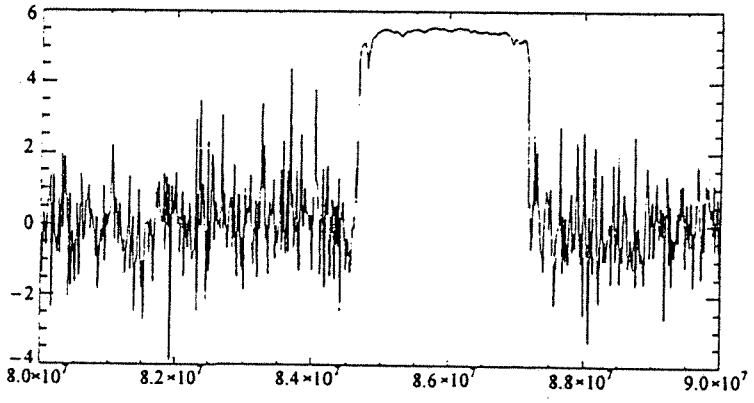

Fig. 2. The part of Fig. 1 with an excursion.

4. Numerical Results

The first data provided by computer simulation of a bottomless system were presented in [8], where Eq. (16) was examined in the bottomless case $\lambda < 0$. The existence of some limits (as $t \to \infty$) was reported. The simulations were continued in order to obtain the information one needs to understand the nature of these limits.

We solved Eq. (16) numerically with $\lambda = -0.06$, using the standard algorithm of the Langevin simulation. The fictitious time step we chose was $\Delta t = 0.01$ and the number of steps was $3 \cdot 10^8$. A typical sample path of the φ_t process is shown in Fig. 1.

To estimate the level of the excursions, notice that if $\Delta t = 0.01$, $\lambda = -0.06$, then the value of

$$|\Delta\varphi_t| \approx |\varphi_t| \exp\left(\frac{\lambda\varphi_t^4}{4}\right)\Delta t + \exp\left(\frac{\lambda\varphi_t^8}{8}\right)\sqrt{2\Delta t}$$

is equal to $1.3 \cdot 10^{-3}$ when $|\varphi_t| = 5$, $8.47 \cdot 10^{-6}$ when $|\varphi_t| = 6$, and $2.13 \cdot 10^{-9}$ when $|\varphi_t| = 7$. Therefore. when $|\varphi_t| \geq 6$, the value of the solution barely changes. That means that in this case, the value of the excursions is approximately six.

An excursion did take place during the simulation shown in Fig. 1. One can see this in Fig. 2, where part of the sample path in Fig. 1 is presented.

It is obvious that an incidental, huge, random peak or a sequence of large random peaks can drive the system to an excursion. The first term on the right-hand side of Eq. (16) returns the process to the origin. Therefore, two quantities are of great interest: the threshold value of the peak that drives the process on an excursion and the relaxation time, which is the length of the period between going on the excursion and returning to the origin.

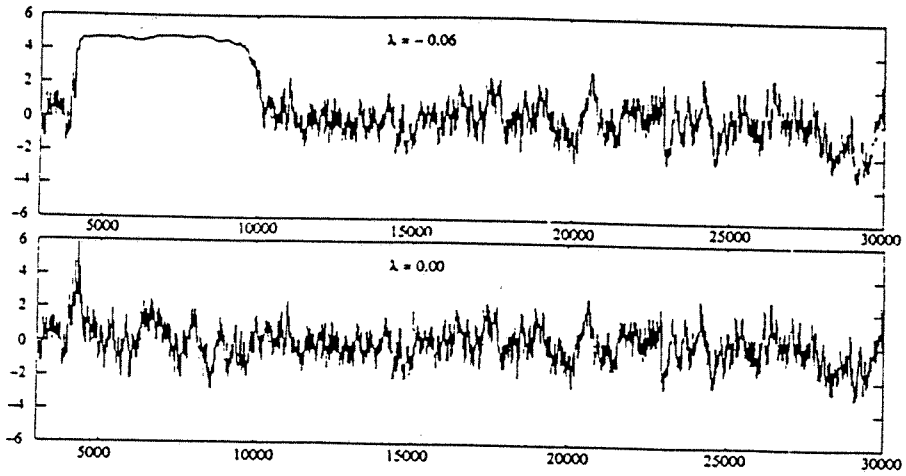

Fig. 3. The φ_t process after a large noise was added.

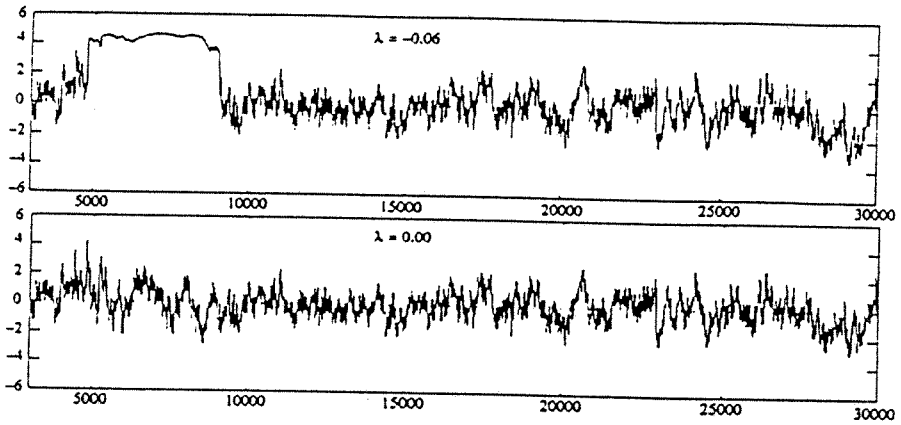

Fig. 4. The φ_t process after a sequence of large noises with intervals of 600 steps was added.

To check the existence of the threshold value for a single, large, random peak, we artificially added Gaussian noise with values larger than 20.0 to w_t. During these numerical simulations, the system often went on excursions and we estimated the threshold value as 30.0. In Fig. 3, the solutions of Eq. (16) with $\lambda = -0.06$ and $\lambda = 0$ are correlated. In both cases, we added a Gaussian process with $\Delta w_t \approx 30$ to w_t. When $\lambda = 0$, the drifting force in (16) plays an important role. Therefore, in this case, the excursions are short. In Fig. 3, bottom, the excursion appears as just a narrow peak. However, when $\lambda = -0.06$, the drifting force is relatively small and an excursion lasts for quite a long time (see Fig. 3, top).

Clearly, there is an extremely small probability that the value of the random noise in the usual numerical simulation takes a value larger than 30.0. Thus, we may confirm that excursions will not occur from a single, huge, random peak.

To estimate the relaxation time, we added an auxiliary Gaussian noise with values about 20.0 to w_t, i.e., lower than the threshold value. This impinging noise was added to the Langevin simulation three times at certain update intervals. Changing these update intervals from 100 to 1000 steps, we can see that the excursion occurs until the update interval becomes 500. In other words, the drift force cannot deal with impinging impulses of such frequency. When the impulses are less frequent, the excursions disappear. It is interesting to notice that when the update intervals are greater than 600, the excursions sometimes appear again.

In Fig. 3, the process of developing an excursion is presented. A random sequence of large noise values causes the system to drift from the origin. One may see that, at the beginning, the process is "trying" to get back, but the next large value of the white noise does not allow the process to return from the excursion.

Let us examine the mathematical expectation $E\varphi_t^{2k}$. To estimate these values, we used different parts

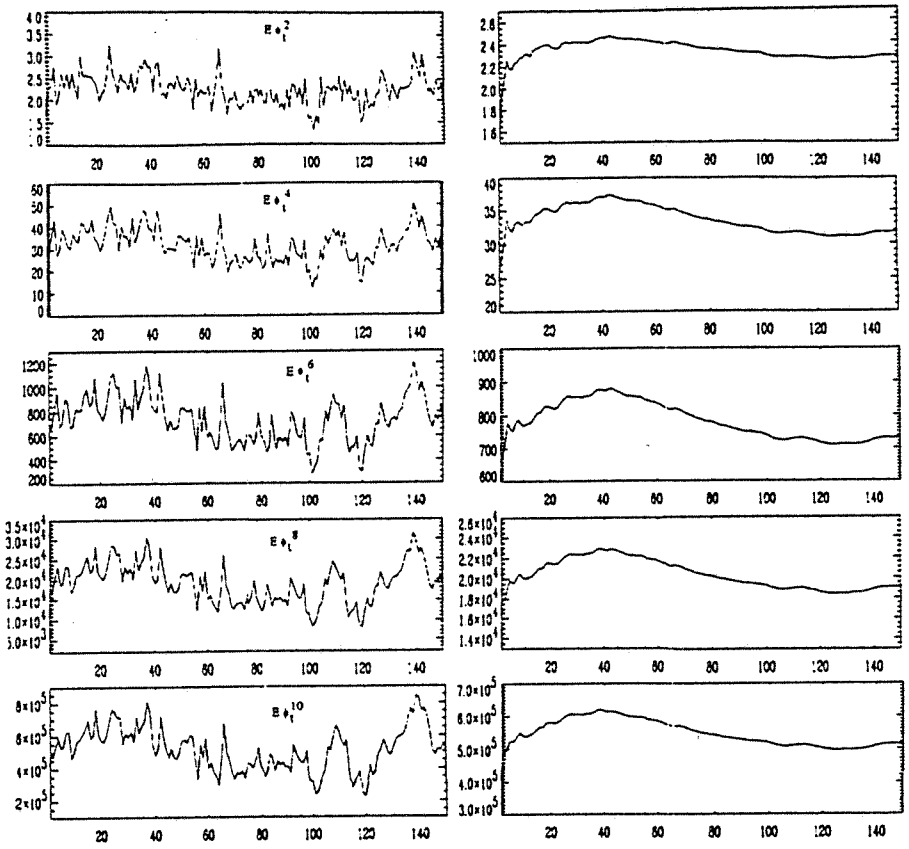

Fig. 5. Mathematical expectations $\mathrm{E}(\varphi_t{}^{2k})$ (left) and their time averages (right) for $k = 1, 2, 3, 4, 5$.

of the trajectory in Fig. 1. These parts were treated as independent sample paths in the same time interval $[0, 150s]$. Results obtained in this way are shown in Fig. 5. Plots of the $t \to \mathrm{E}\varphi_t^{2k}$ functions are on the left and it is apparent that these functions are very chaotic. This agrees with the above-stated fact that they do not have a limit when $t \to \infty$. However, the functions

$$t \to \frac{1}{t} \int_0^t \mathrm{E}\varphi_s^{2k}\, ds \tag{22}$$

seem to have limits when $t \to \infty$ (see Fig. 5, right).

In Fig. 6, the graph of the function

$$t \to \frac{1}{t} \int_0^t \varphi_s^2\, ds$$

is shown, where φ_t is the same as in Fig. 1. This figure supports our idea that the limits

$$\lim_{t\to\infty} \frac{1}{t} \int_0^t \varphi_s^{2k}\, ds$$

may exist with a probability 1 and that we have no need to take the expectation values as in (22).

To compare the Borel summation and stochastic approaches, we calculate the λ-dependence of G_2 in the range $-0.08 < \lambda < 0.00$. Such a dependence, obtained in the stochastic approach and based on time averages, is presented in [8]. Among the four values that $G_2(\lambda)$ takes on the cuts, we chose those with a positive imaginary part. We found that the values $\mathrm{Re}\, G_2(\lambda) + \mathrm{Im}\, G_2(\lambda)$ are almost the same as those obtained by the stochastic approach.

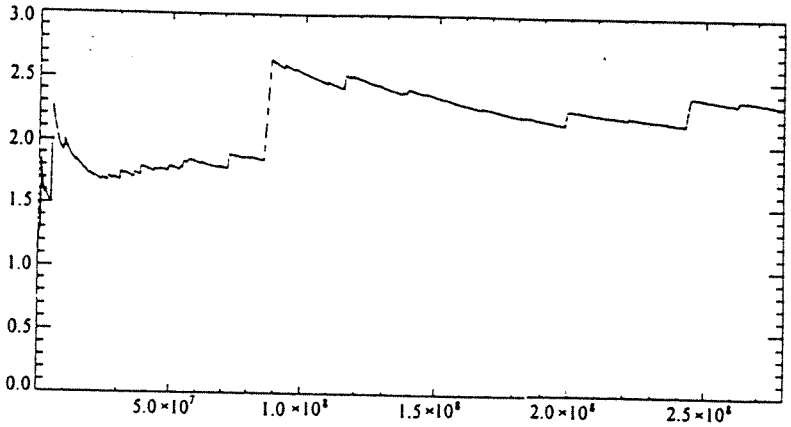

Fig. 6. Time average of the process ${\varphi_t}^2$ for the sample path from Fig. 1.

5. Conclusions

We have shown that when employing the Borel summation method and the stochastic approach, one may obtain some results when calculating integrals like (3) in the bottomless case. The Borel method works for any value of the coupling constant λ and order n of the Schwinger function. However, the method does not give uniquely definite results and one has to combine four values for each λ and n. The sum of the real and imaginary parts of the value G_n takes on one edge of the cut appears to be a good candidate.

The stochastic approach, based on the kerneled Langevin equation, reproduces the distribution $\exp[-\varphi^2/2 - \lambda\varphi^4/4]$ for any value of λ. The ergodic equalities between the expectations and time averages are not valid in the bottomless case; the Schwinger functions appear to be the time averages.

The excursions above a high level are important in the bottomless case. The probability of excursions increases when $(-\lambda)$ increases. Therefore, the case of large $(-\lambda)$ is more suitable for computer simulations than that of small $(-\lambda)$, where the excursions are rare and one runs the risk of losing their contributions. In (21), neglecting the excursions is equivalent to using a cut-off for the values of φ. Relation (21) can be used to test the accuracy of the calculations.

The ambiguity of the Borel summation method appears to be related to the possibility of using different kernels in the stochastic approach. It would be interesting to find an exact form of such a relationship. After that, one might initiate a study of the matrix model with $N > 1$. The first results obtained by stochastic simulation are presented in [9]. Also, the study of an anharmonic oscillator with different values for the coupling constant is of great interest. This model has been examined by the Borel summation method and its treatment by stochastic quantization would be useful in understanding the bottomless system.

This paper was prepared in the framework of the Japan Society for the Promotion of Science project of the Japan–Former Soviet Union scientific collaboration. The financial support of the JSPS is gratefully acknowledged.

REFERENCES

1. S. Graffi, V. Grecchi, and B. Simon, *Phys. Lett. B*, **32**, 631–634 (1970).
2. J.-P. Eckmann, J. Magnen, and R. Seneor, *Commun. Math. Phys.*, **39**, 251–271 (1975).
3. J. Avron, I. Herbst, and B. Simon, "Schrödinger operators with magnetic fields," Preprint, Princeton Univ. (1977).
4. A. Erdélyi et al. (eds.), *Higher Transcendental Functions* (Based on notes left by H. Bateman), McGraw-Hill, New York (1953).
5. R. Z. Has'minskiĭ, *Stochastic Stability of Differential Equations*, Sijthoff & Nordhoff, Alphen Van den Rijn, Rockville (1980).
6. M. Namiki, *Stochastic Quantization*, Springer (1992).
7. J. D. Breit, S. Gupta, and A. Zaks, *Nucl. Phys. B*, **233**, 61 (1984).
8. S. Tanaka, M. Namiki, I. Ohba, M. Mizutani, N. Komoike, and M. Kanenaga, *Phys. Lett. B*, **288**, 129 (1992).
9. M. Kanenaga, M. Mizutani, M. Namiki, I. Ohba, and S. Tanaka, *Prog. Theor. Phys.*, **91**, 599–610 (1994).

ELSEVIER

Nuclear Physics B 485 [FS] (1997) 727–746

NUCLEAR PHYSICS B

Universality and scaling in short-time critical dynamics

K. Okano [a], L. Schülke [b,1], K. Yamagishi [a], B. Zheng [b]

[a] *Tokuyama University, Tokuyama-shi, Yamaguchi 754, Japan*

[b] *Universität – GH Siegen, D-57068 Siegen, Germany*

Received 12 January 1996; revised 10 October 1996; accepted 29 October 1996

Abstract

The short-time scaling behaviour of the critical dynamics for the two-dimensional Ising model and Potts model are investigated with both the heat-bath and the Metropolis algorithm. Special attention is drawn to universality. We observed that the microscopic time scale t_{mic} after which the universal scaling behaviour appears is not always negligibly small. Taking carefully the effect of t_{mic} into account, the critical exponents are extracted from the power law behaviour of the observables in the beginning of the time evolution. All the results are consistent and therefore universality and scaling are confirmed.

PACS: 64.60.Fr; 02.70.Lq; 05.70.Jk; 64.60.Ht

Keywords: Short-time dynamics; Ising system; Critical phenomena; Monte Carlo method

1. Introduction

It is well known that the critical behaviour of a statistical system in and near equilibrium is characterized by a universal scaling form. This is more or less due to the *infinite* spatial and time correlation lengths. It has long been discussed whether universal behaviour may also be found in a system far from equilibrium.

Let us consider that the Ising model initially in a random state with a small magnetization is suddenly quenched to the critical temperature and then evolves according to the dynamics of model A. Janssen, Schaub and Schmittmann [1] have recently argued with the $O(N)$ vector model by an ϵ-expansion up to two-loop order that, besides the

[1] E-mail: schuelke@pollux.physik.uni-siegen.de.

PII S0550-3213(96)00615-3

well-known universal behaviour in the long-time regime, there exists another universal stage of the relaxation *at macroscopic early times*, the so-called critical initial slip, which sets in right after the microscopic time scale t_{mic}. The authors predicted that the magnetization undergoes a *critical initial increase*, and introduced a new independent dynamic critical exponent θ to describe the power law increase of the magnetization.

So far numerical simulations support the above predictions. Previously θ has been measured with Monte Carlo simulation in the two-dimensional Ising model somehow *indirectly* from the power law decay of the autocorrelation [2,3], and recently in the three-dimensional Ising model and the two-dimensional Potts model *directly* from the power law increase of the magnetization [4,5]. More interestingly, based on the scaling relation in the initial stage of the time evolution, a new promising way for measuring also the exponents z, β and ν has been proposed [6–8]. This indicates a possible broad application of the short-time dynamics since the universal behaviour of the short-time dynamics is found to be quite general [9–14].

Even though the short-time dynamic scaling behaviour has numerically been studied by several authors, up to now one important question remains untouched: are the exponents extracted from the short-time dynamics really independent of algorithms (heat bath, Metropolis etc.) and/or the lattice type (square, triangular etc.), and so on? In other words, *is the short-time scaling behaviour really universal?* Giving a rigid and decisive answer to this question is overdue. In this paper, we will show an interesting numerical evidence for the universality by the comparison of the results obtained from the heat-bath and the Metropolis algorithm. This confidently serves as the first step approach in this direction.

In the literature, almost all the numerical simulations of the short-time dynamics have been performed with the heat-bath algorithm. In this case, the power law behaviour of the magnetization surprisingly shows up almost from the first Monte Carlo time step. We claim in this paper that this happened rather by chance and that it is not always the case. Even though universal behaviour is expected in the *macroscopic early time*, in general, the dynamic system needs a certain microscopic time period to get rid of the microscopic short-wave effects and to enter the macroscopic quasi-stable state. Such a time period is called the microscopic time scale t_{mic}. It is only for $t > t_{mic}$ that the exponents extracted from the short-time dynamics will be universal, i.e. will be independent of the algorithms and other microscopic details. We will show that for the Metropolis algorithm the microscopic time scale is around $t_{mic} \sim 20$ and is not as small as for the heat-bath algorithm. For the heat-bath algorithm, it is only a good luck that t_{mic} is negligibly small. This also shows, however, that for the numerical study of the short-time dynamics the heat-bath algorithm is more efficient.

In the first part of this paper, therefore, we present numerical results for the two-dimensional Ising model for both the heat-bath and Metropolis algorithm in order to understand the universality for short-time dynamics. It turns out that the behaviour of the magnetization, autocorrelation and the second moment depend, sometimes seriously, on the dynamics when t is small in the microscopic sense. However, we observe a clear evidence for universality after the microscopic time scale t_{mic}, which is big enough

in the microscopic sense, but is still in the macroscopic early time regime. The precise knowledge of $t_{\rm mic}$ is essential for the high precision measurement of the critical exponents.

In the second part of this paper we further analyse the short-time critical dynamics for the two-dimensional Potts model. Preliminary results for the Potts model with the heat-Bath algorithm have already been published in Ref. [5]. In the present paper the results will be refined by taking the microscopic time $t_{\rm mic}$ into account carefully. Furthermore the data have been extended to bigger lattice size $L = 576$ for the simulation of $m_0 = 0.0$ and smaller initial magnetization $m_0 = 0.02$ for the measurement of θ in order to clarify some unclear points with respect to the finite size effect and the finite m_0 effect. Among the values of z for the Potts model given in the literature [15–18], our results confidently support relatively smaller ones [15,16].

Our paper also aims to present a systematic description for the numerical simulation of the short-time dynamics since almost all the relevant existing papers are of letter type. Our detailed analysis reveals the fine structure of the short-time scaling behaviour for the critical dynamics and demonstrates how one should confidently extract the critical exponents.

In Section 2 we briefly recapitulate the scaling behaviour for the short-time dynamics, which will serve as the theoretical base of the numerical simulation. In Section 3 we describe the result of a simulation for the Ising model in two dimensions, concentrating our attention to universality. In Section 4 the results for the three state Potts model are presented. Conclusion and further remarks are given in Section 5.

2. Scaling for the short-time dynamics

Let us consider a dynamic system of model A. Janssen, Schaub and Schmittmann have shown [1] that when a system initially in a state with very high temperature $T \gg T_c$ is suddenly quenched to the critical temperature and then evolves according to a certain dynamics, besides the well-known universal behaviour in the long-time regime, there emerges another universal stage of the dynamic relaxation at the *macroscopic short-time regime*, which sets in right after a microscopic time scale $t_{\rm mic}$. For the $O(N)$ vector model the renormalization of the Langevin dynamics with initial conditions has been investigated with ϵ-expansion up to two-loop order. An interesting observation is that a new divergence is induced in the short-time dynamics which should be renormalized by the initial magnetization. Taking this point into account, a generalized dynamic scaling relation has been derived,

$$M^{(k)}(t, \tau, m_0) = b^{-k\beta/\nu} M^{(k)}(b^{-z}t, b^{1/\nu}\tau, b^{x_0}m_0), \tag{1}$$

where $M^{(k)}$ is kth moment of the magnetization, t is the dynamic relaxation time, τ is the reduced temperature, the parameter b represents the spatial rescaling factor, and in addition x_0 is the anomalous dimension of the initial magnetization m_0. It is shown that

x_0 is *a new independent exponent*, i.e. it can not be expressed by other known critical exponents.

As an example, let us now consider the time evolution of the magnetization in the initial stage of the dynamic relaxation. From the above scaling relation (1), taking $\tau = 0$ and $b = t^{1/z}$,

$$M(t, m_0) = t^{-\beta/\nu z} M(1, t^{x_0/z} m_0). \tag{2}$$

In our notation $M \equiv M^{(1)}$ and the argument τ has been omitted. Assuming the initial magnetization m_0 to be small, the time evolution of the magnetization may be expanded according to m_0

$$M(t, m_0) = m_0 F(t) + O(m_0^2). \tag{3}$$

Here the condition $M(t, m_0 = 0) \equiv 0$ has been used. From Eqs. (2) and (3) one can easily realize that the time evolution of the magnetization obeys a power law

$$M(t) \sim m_0 t^{\theta}, \tag{4}$$

where the exponent θ is related to x_0 by

$$\theta = (x_0 - \beta/\nu)/z. \tag{5}$$

Here we should stress that the power law behaviour is valid only in case that $t^{x_0/z} m_0$ is also small enough. Therefore the universal behaviour shown in (4) is expected in the initial stage of the time evolution. Its time scale is $t_0 \sim m_0^{-z/x_0}$. However, in the limit of $m_0 = 0$ the time scale t_0 goes to infinity. Hence the initial condition can leave its trace even in the long-time regime [19,12,20]. Interestingly, for the $O(N)$ vector model ($N = 1$ corresponds to the Ising model) it has been shown by ϵ-expansion that $x_0 > \beta/\nu$ and therefore $\theta > 0$, i.e. the magnetization undergoes a *critical initial increase*. This has also been confirmed by numerical simulation for the three-dimensional Ising model directly and also by the study of damage spreading [21].

As the spatial correlation length in the beginning of the time evolution is small, for a finite system of dimension d with lattice size L the second moment $M^{(2)}(t, L) \sim L^{-d}$. From the finite size scaling one can deduce

$$M^{(2)}(t) \sim t^{(d-2\beta/\nu)/z}. \tag{6}$$

Furthermore careful scaling analysis shows that auto-correlation also decays by a power law [9]

$$A(t) \sim t^{-d/z+\theta}. \tag{7}$$

The new dynamic exponent θ enters also the auto-correlation. Actually the first numerical estimation of θ is from the measurement of the exponent $\theta - d/z$ [2,3]. Taking the exponent z as an input, one obtains θ. However, usually z is not known so accurately. Since θ is normally much smaller than z as well as $-d/z + \theta$, a small relative error of z and $-d/z + \theta$ may induce a big error for θ.

Therefore our strategy is that we first measure the exponent θ directly from the power law increase of the magnetization, then taking it as an input we estimate the exponent z from the auto-correlation, and with z in hand we finally obtain the static exponent $2\beta/\nu$ from the second moment. Such a procedure can provide strong confirmation for the scaling relation for the short-time dynamics.

Traditionally the exponent z is defined in the long-time regime of the dynamic process and normally measured from the exponential decay of the auto-correlation or the magnetization of the systems. This measurement is difficult due to critical slowing down. However, if we can obtain θ from the direct measurement of the initial increase of the magnetization (4), z obtained from the scaling behaviour of the auto-correlation in (7) can be quite rigorous. One may also expect that the measurement is to some extent free from critical slowing down, since all of these quantities are measured in the short-time regime of the dynamic process.

3. The Ising model and universality

In this section we analyse the short-time dynamics of the Ising model for the heat-bath and the Metropolis algorithm and investigate the universality of the short-time dynamics with these two algorithms. In the same time we try to formulate a proper way to measure the critical exponent taking into account the effects of the microscopic time scale t_{mic}.

The Hamiltonian for the Ising model is

$$H = J \sum_{\langle ij \rangle} S_i S_j , \qquad S_i = \pm 1 , \tag{8}$$

with $\langle ij \rangle$ representing nearest neighbours. In equilibrium the Ising model is exactly solvable. The critical point locates at $J_c = \log(1 + \sqrt{2})/2$. In principle any type of dynamics can be given to the system to study the non-equilibrium evolution process. In this paper we concentrate our attention on the Monte Carlo heat-bath and the Metropolis algorithm, both of which belong to the dynamics of model A.

3.1. Magnetization

We study the short-time behaviour of the dynamical process starting from an initial state with *zero correlation length and small magnetization*. Such initial configurations can easily be generated numerically [4,5]. Starting from those initial configurations, the system is updated both with the heat-bath and Metropolis algorithm. We measure the time evolution of the magnetization

$$M(t) = \frac{1}{N} \left\langle \sum_i S_i(t) \right\rangle . \tag{9}$$

where N is the number of the lattice sites and the average $\langle \ldots \rangle$ is taken over the independent initial configurations and the random force. The total number of independent

initial configurations is 150 000 for $m_0 = 0.08, 0.06$ and 0.04 and 300 000 for $m_0 = 0.02$. Errors are estimated by dividing the data into five groups.

In Fig. 1a and 1b the time evolution of the magnetization is displayed in double log scale with $m_0 = 0.02$ for different lattice sizes for the heat-bath and the Metropolis algorithm, respectively. For the heat-bath algorithm, one can clearly see that the initial *power law* increase of the magnetization starts from a very early stage of the time evolution, i.e. the microscopic time scale t_{mic} is negligibly small. On the other hand, for the Metropolis algorithm, this is not the case. The power law increase of the magnetization becomes stable only after certain time steps, say $t \sim 20$ to 30. In other words, for the Metropolis algorithm $t_{\text{mic}} \sim 20$ to 30, which is much bigger than that for the heat-bath algorithm. In order to see this more clearly, we plot in Fig. 2 the exponent θ as a function of the time t for both the heat-bath and the Metropolis algorithm from $m_0 = 0.02$ to 0.08. The lattice size $L = 128$ has been used. Here, "θ at time t" is measured from the slope of the curve in the time interval of $[t, t + 15]$ by least square fitting.

As expected, the exponent θ for the heat-bath algorithm is quite stable from the very beginning of the time evolution but not that for Metropolis. Taking into account the errors as well as the fluctuation along the time direction, however, the exponents θ from both algorithms become the same after $t > t_{\text{mic}} \sim 30$. This is a real indication of the universality in the short-time dynamics.

From these results, a criterion to measure the critical exponent θ and also other exponents can be obtained.

(i) We first scan the data by the exponent measured at each time t by least square fitting in the time interval of $[t, t + 15]$. We call this "15-scan" in the following. Of course, the number of data for the least square fit can differ from 15 which is used here.

(ii) Using the figure obtained from the 15-scan, we can estimate t_{mic} from which the exponent becomes stable. If we perform a simulation with different algorithms, we can compare these results and see that universality is valid after the microscopic time t_{mic}.

(iii) Finally we perform the least square fit in the time interval of $[t_{\text{mic}}, T]$ to obtain the final values for the exponents. Here T can normally be the maximum updating time where finite size effects and the finite m_0 effect have not shown up. But sometimes we may take T a bit smaller in order to escape big fluctuations due to the lack of statistics. This can be judged by an inspection of the result of the 15-scan.

In Fig. 2. one can observe a tendency that t_{mic} decreases as m_0 gets smaller. We should also stress that the errors estimated here can not completely represent the fluctuations in the time direction due to the large time correlation length and also other systematic errors, e.g. those from the random numbers. In Table 1, results for θ measured from a time interval $[30, 100]$ are listed. A detailed analysis of the data reveals that the finite size effect is quite small for a lattice size $L = 128$.

From $m_0 = 0.08$ down to $m_0 = 0.02$ the measured θ shows a smooth linear increase. By definition the exponent θ should be measured in the limit of $m_0 = 0$. Following the procedure in the previous paper [5] we have carried out a linear extrapolation to $m_0 = 0$ and listed the results also in Table 1. The value $\theta = 0.191(1)$ from the heat-bath algorithm is well consistent with the value $\theta = 0.191(3)$ obtained from

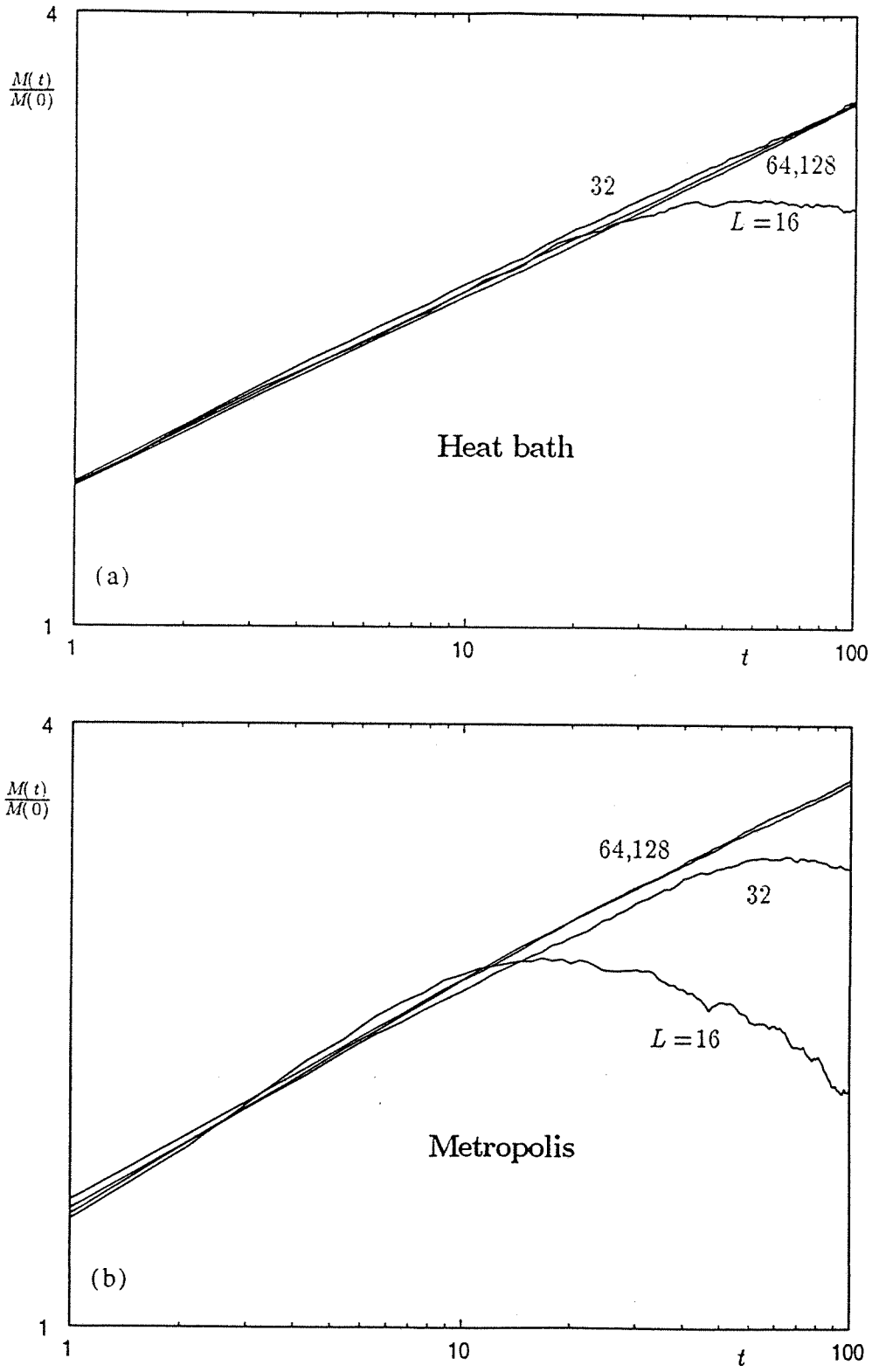

Fig. 1. Time evolution of the magnetization in double log scale for the Ising model with $m_0 = 0.02$ for the heat-bath algorithm and for the Metropolis algorithm.

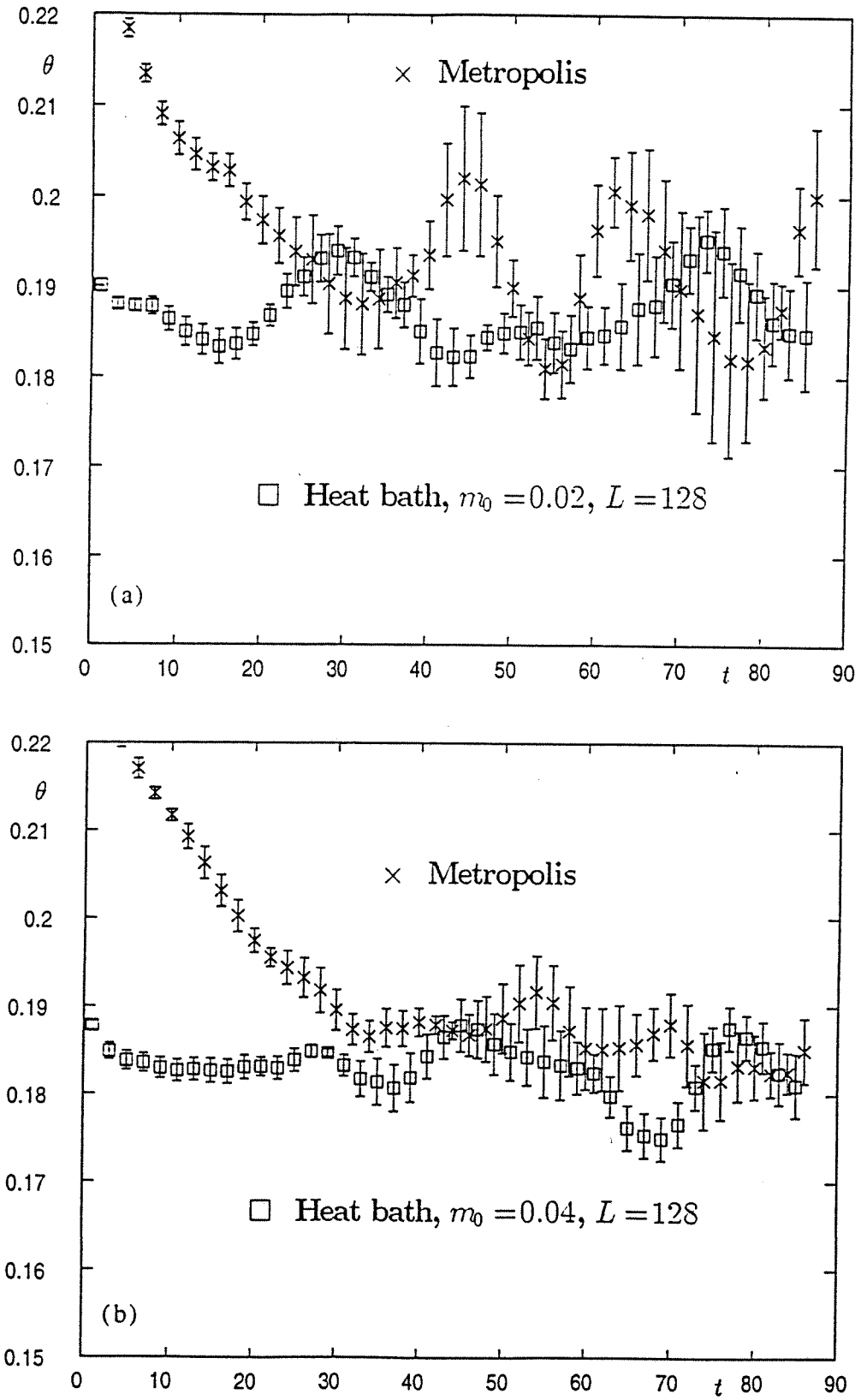

Fig. 2. θ vs. t for the Ising model with $m_0 = 0.02$, $m_0 = 0.04$, $m_0 = 0.06$ and $m_0 = 0.08$.

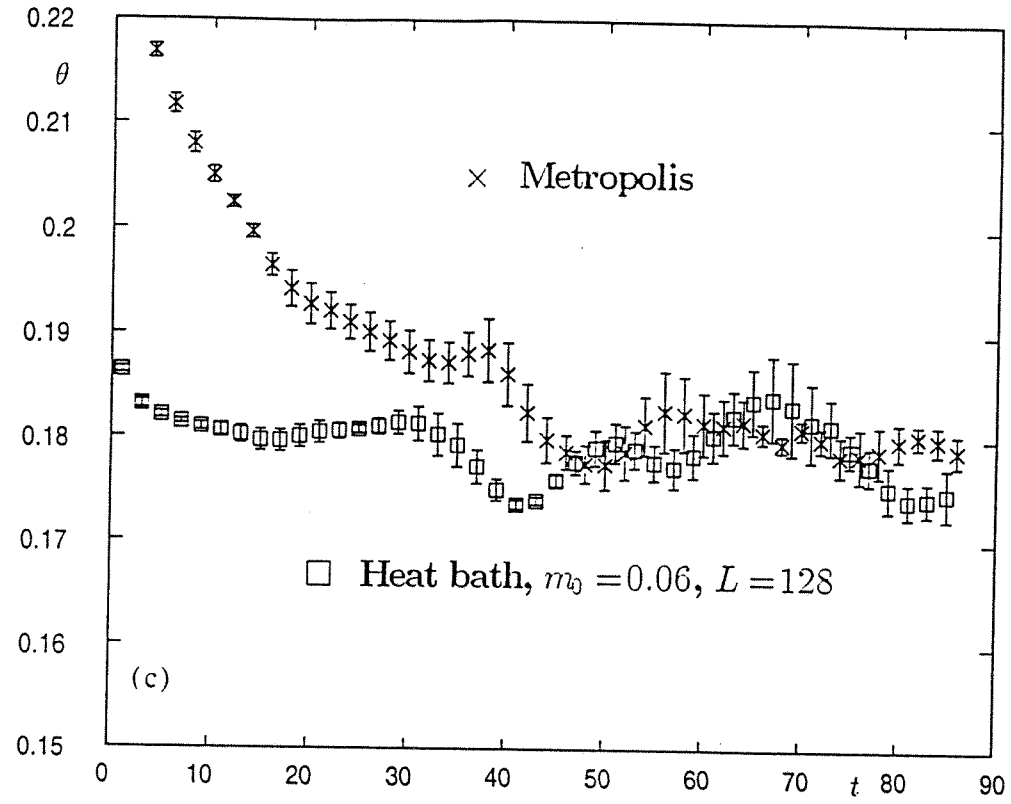

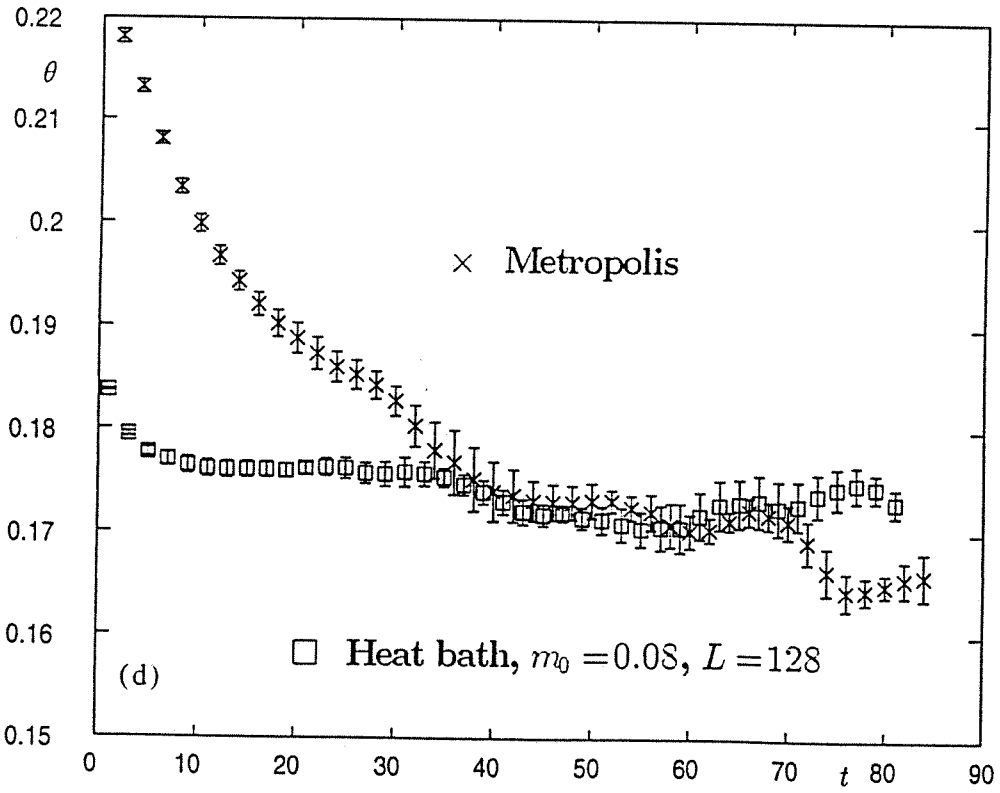

Fig. 2 — continued.

Table 1
The short-time dynamic exponent θ measured for lattice size $L = 128$ with different initial magnetization for the Ising model

m_0	0.08	0.06	0.04	0.02	0.00
HeatB	0.173(1)	0.179(1)	0.183(1)	0.187(1)	0.191(1)
MetroP	0.173(1)	0.182(1)	0.187(1)	0.192(1)	0.197(1)

damage spreading [21] and those obtained from auto-correlation before [2,3]. For the Metropolis algorithm, our first direct measurement $\theta = 0.197(1)$ is very close to that for the heat-bath algorithm and gives strong support for universality. The slight difference of θ for the heat-bath and the Metropolis algorithm may arise from the finite size effect, finite m_0 effect or other systematic errors. To check this point, simulations with higher statistics for smaller m_0 and bigger lattice size or even for longer updating time may be needed.

In closing this subsection, we would like to mention that the numerical values for the exponent θ obtained above are roughly consistent with that extrapolated from the perturbative calculations based on the continuum ϕ^4 theory [1], in one-loop $\theta = 0.167$ and in two-loop $\theta = 0.356$. Here one should remember that the perturbative theory is only valid for dimensions bigger than two and smaller than four and therefore the coincidence cannot be too precise in two dimensions.

3.2. Auto-correlation

Now we set $m_0 = 0$. The auto-correlation is defined as

$$A(t) = \frac{1}{N}\left\langle \sum_i S_i(0) S_i(t) \right\rangle . \tag{10}$$

We have performed simulations with both the heat-bath and Metropolis algorithm for lattice size $L = 256$. The number of independent initial configurations for the average is 35 000.

In order to see the universality and the possible effect of t_{mic} as well as the fluctuation in the time direction, we again perform the 15-scan and display in Fig. 3 the exponent $\theta - d/z$ as a function of time t for both the heat-bath and the Metropolis algorithm.

After a microscopic time scale $t_{\mathrm{mic}} \sim 30$, the results from both algorithms agree well and are presenting a quite stable power law behaviour. This again supports universality. Within the errors both algorithms give almost the same results. However, the error for Metropolis is much bigger than that for the heat-bath algorithm.

In Table 2 the exponents $d/z - \theta$ measured from the time interval [30, 100] are listed. They are consistent with the previous measurement [22], but the errors are much smaller. The dynamic exponent z obtained by taking θ measured in the previous subsection as input are also given in Table 2. For the heat-bath algorithm, the value $z = 2.155(3)$ is in good agreement with $z = 2.153(2)$ measured from the finite size scaling of the

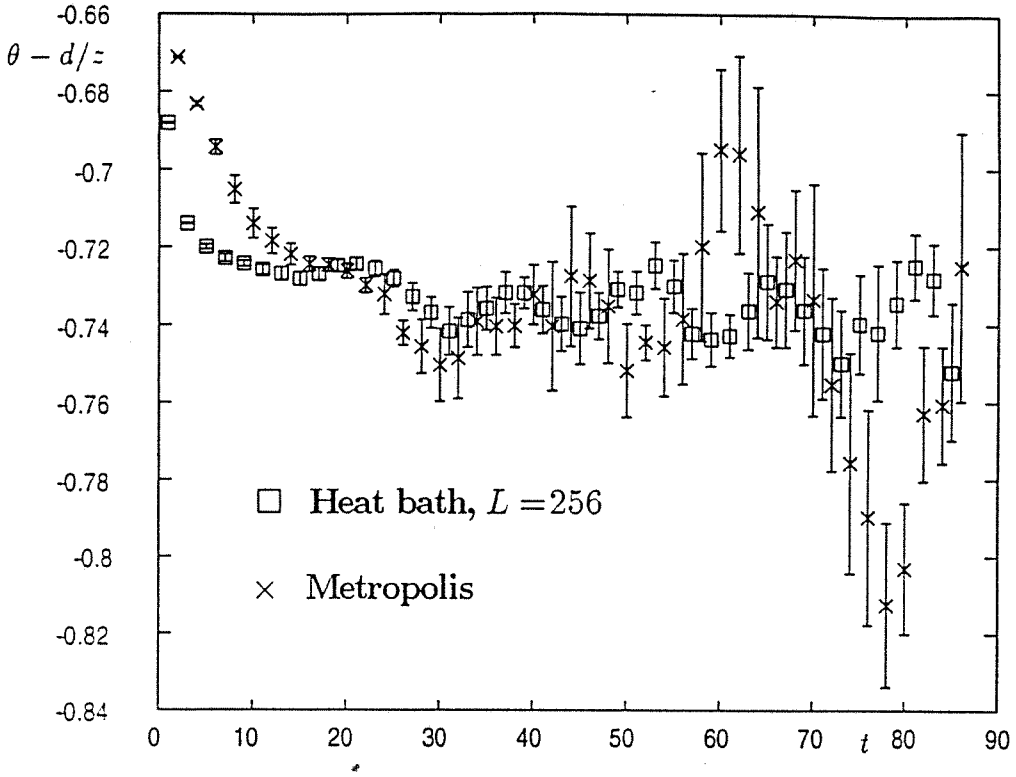

Fig. 3. $\theta - d/z$ vs. t for the Ising model.

Table 2
The exponents measured for lattice size $L = 256$ with initial magnetization $m_0 = 0.0$ for the Ising model

	$d/z - \theta$	z	$(d - 2\beta/\nu)/z$	$2\beta/\nu$
HeatB	0.737(1)	2.155(03)	0.817(7)	0.240(15)
MetroP	0.739(5)	2.137(11)	0.819(5)	0.250(14)

Binder cumulant [7]. The value $z = 2.137(11)$ for the Metropolis algorithm is slightly smaller but roughly consistent within the errors. Actually in Ref. [7], depending on the observables and the dynamic processes used for estimating z, the values for z from the finite size scaling are also varying within 1%. To get more accurate z still requires high precision numerical measurement.

3.3. Second moment

For $m_0 = 0$, the second moment is defined by

$$M^{(2)}(t) = \frac{1}{N^2} \left\langle \left[\sum_i S_i(t) \right]^2 \right\rangle . \tag{11}$$

For the heat-bath algorithm the exponent $(d - 2\beta/\nu)/z$ is quite stable after $t_{\mathrm{mic}} \sim$ 20 to 30. However, for the Metropolis algorithm, t_{mic} seems to be somewhat bigger,

$t_{\rm mic} \sim 60$. In order to obtain more reliable results, we have extended the number of time steps for the Metropolis algorithm up to 150. In Table 2 the measured values for $(d - 2\beta/\nu)/z$ together with the exponent $2\beta/\nu$ deduced by taking the value of z from the previous subsection as input are given. All the results are consistent and are confirming universality.

We should point out that the determination of the exponent $2\beta/\nu$ is not very accurate here since the exponent $2\beta/\nu$ is much smaller than d and z, and therefore small relative errors in z and $(d - 2\beta/\nu)/z$ will induce big errors for $2\beta/\nu$.

Summarizing this section, we have investigated the universality in short-time dynamics for the Ising model. In the numerical simulations, we observed that the microscopic time scale $t_{\rm mic}$ is not always negligibly small. Universal behaviour appears only after $t > t_{\rm mic}$. We have also found that $t_{\rm mic}$ is different for the different algorithms, Metropolis or heat-bath algorithm. Precise knowledge about $t_{\rm mic}$ will be very important in high precision measurements of the critical exponents in short-time dynamics.

4. The Potts model

In order to confirm the picture for the universality drawn in the last section, further investigations for different models are needed. In this section we present numerical results for the short-time dynamics of the Potts model. Two of us (L.S. and Z.B.) have already reported preliminary results in Ref. [5]. In that letter, however, the simulation has exclusively been performed with the heat-bath dynamics and for the measurement of the exponent θ the smallest initial magnetization is taken to $m_0 = 0.04$. The effect of the microscopic time scale $t_{\rm mic}$ has not been considered seriously. On the other hand, in the measurement of the auto-correlation an extrapolation to infinite lattice size was carried out. It is not so clear whether this extrapolation is really necessary for the lattice size already up to $L = 288$. Therefore the purpose of this section is to give final numerical values for the critical exponents of the Potts model, taking carefully the effect of the microscopic time $t_{\rm mic}$ into account and using bigger lattices and smaller m_0 with increasing statistics.

The Hamiltonian for the q state Potts model is given by

$$H = J \sum_{\langle ij \rangle} \delta_{\sigma_i,\sigma_j}, \qquad \sigma_i = 1, \ldots, q, \tag{12}$$

where $\langle ij \rangle$ represents nearest neighbours. It is known that the critical points locate at $J_c = \log(1 + \sqrt{q})$. The Ising model is the two-state ($q = 2$) Potts model. In this section, we investigate the three-state ($q = 3$) Potts model in two dimensions.

4.1. Magnetization

We measure the time evolution of the magnetization defined as

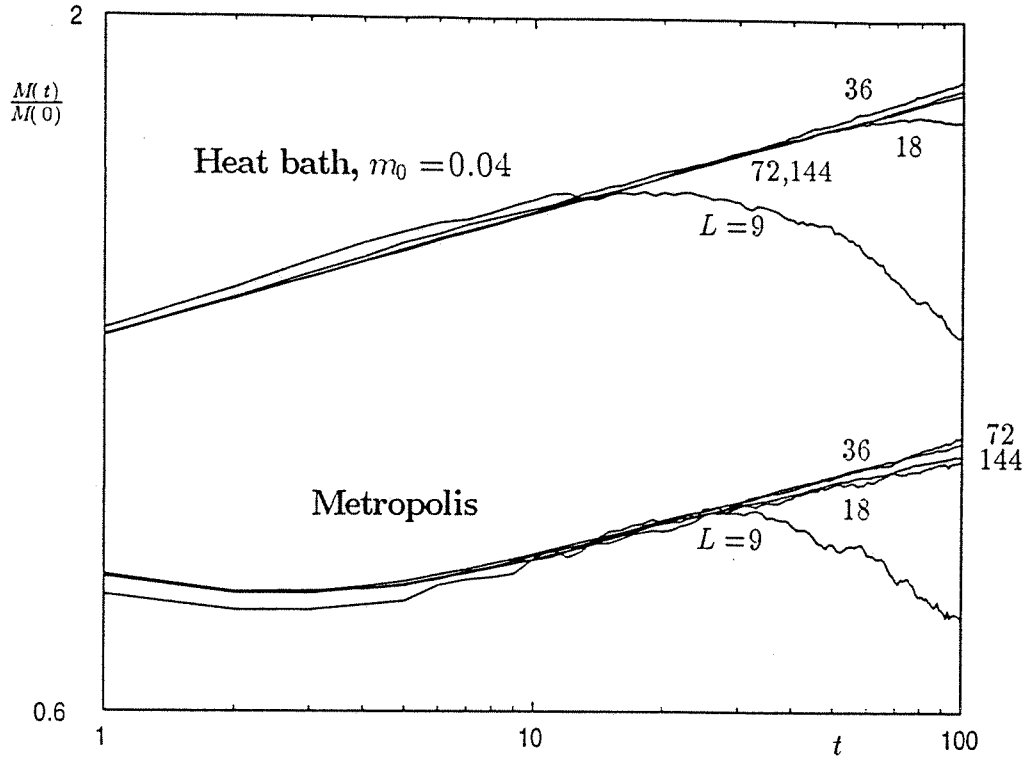

Fig. 4. The time evolution of the magnetization in double log scale for the Potts model with $m_0 = 0.04$.

$$M(t) = \frac{3}{2N}\left\langle \sum_i \left(\delta_{\sigma_i(t),1} - \frac{1}{3}\right)\right\rangle. \tag{13}$$

The total number of the independent initial configurations used for taking the average is 80 000 for $m_0 = 0.06$ and 0.08 and 600 000 for $m_0 = 0.02$ and 0.04. Similar to the case of the Ising model, errors are estimated by dividing the data into two or four groups.

In Fig. 4 the time evolution of the magnetization is displayed in double log scale with initial value $m_0 = 0.04$ for different lattices size and for both the heat-bath and Metropolis algorithm. Somewhat different from the case of the Ising model, the view of the curves from the heat-bath and Metropolis algorithm appears very different. For the curves from the heat-bath algorithm the power law behaviour starts right at the very beginning of the time evolution as in the case of the Ising model. This means the microscopic time scale t_{mic} is negligible. However, for the Metropolis algorithm the magnetization first decreases and then increases after some time steps. Later analyses show that the power law behaviour becomes stable after around 20 updating time steps, i.e. $t_{\text{mic}} \sim 20$.

As mentioned above, in Ref. [5] the simulation was carried out using the heat-bath algorithm only. Due to the fact that the error at the beginning of the time evolution is the smallest, the exponent has been measured from the first 15 time steps only. However, the results of the simulation for the Metropolis algorithm indicate that one should carefully analyse the data, with special attention to the effect of t_{mic}. We plot

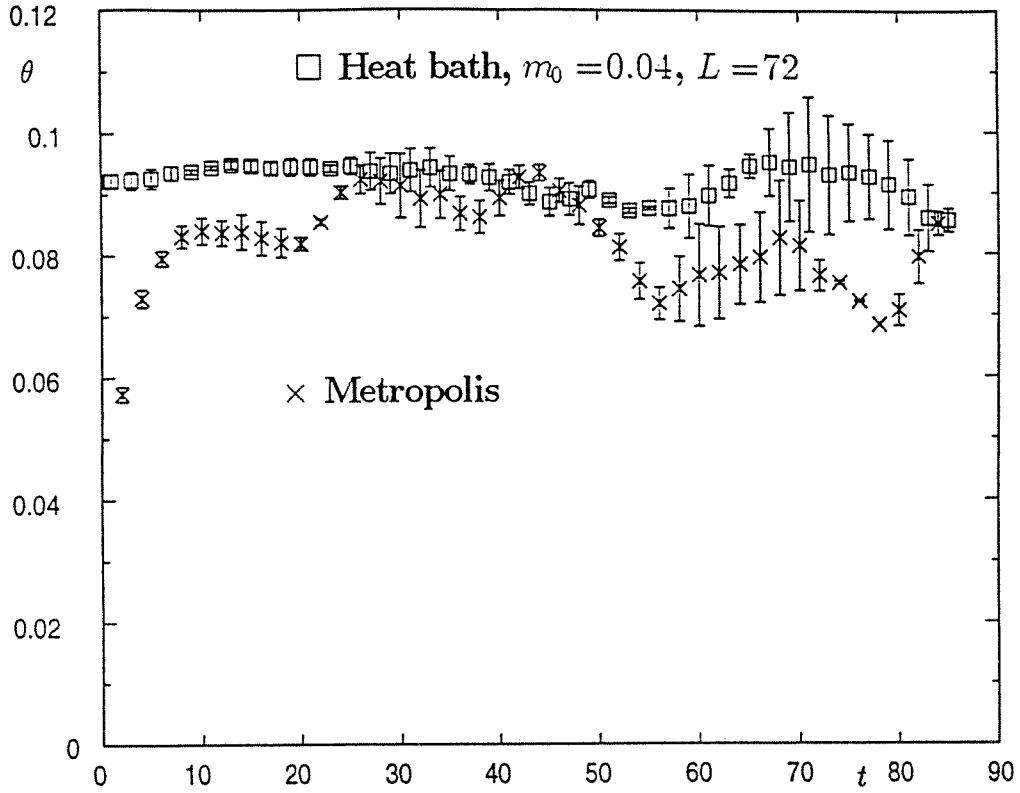

Fig. 5. θ vs. t for the Potts model with $m_0 = 0.04$.

in Fig. 5 the exponent θ vs. t, obtained by the 15-scan for both the heat-bath and Metropolis algorithm with initial magnetization $m_0 = 0.04$. It is clear that θ from the heat-bath algorithm is quite stable from the very beginning of the time evolution but for the Metropolis this is apparently not the case. However, as was the case of the Ising model, the exponent θ from both the heat-bath and Metropolis algorithms coincide after $t > t_{\text{mic}} \sim 20$, showing again the universality in short-time dynamics.

The reason why for the Metropolis algorithm the magnetization decreases at the very beginning of the time evolution is not clear to us. However, the decline only lasts for a few Monte Carlo time steps. As discussed in Section 1, we believe that this is a typical microscopic behaviour within the microscopic time scale t_{mic}. Immediately after the decrease, however, the magnetization increases quickly and a power law universal behaviour is soon stabilized. This strongly shows that there exists universality in the short-time dynamics. Here it should also be stressed that the non-universal behaviour within the microscopic time scale t_{mic} can, in general, not be investigated in continuum models as e.g. the ϕ^4 theory corresponding to the Ising model, since in such a continuum model the information within the microscopic time scale has already been lost. For the Potts model, the corresponding continuum model has even not yet been found.

In Table 3 the values of θ measured from the time interval [20, 100] are listed. In principle for the heat-bath algorithm the measurement may be carried out from the

Table 3
The short-time dynamic exponent θ measured for lattice size $L = 72$ with different initial magnetization for the Potts model

m_0	0.08	0.06	0.04	0.02	0.00
HeatB	0.110(1)	0.100(1)	0.092(2)	0.084(3)	0.075(3)
MetroP	0.100(1)	0.092(1)	0.084(1)	0.077(2)	0.070(2)

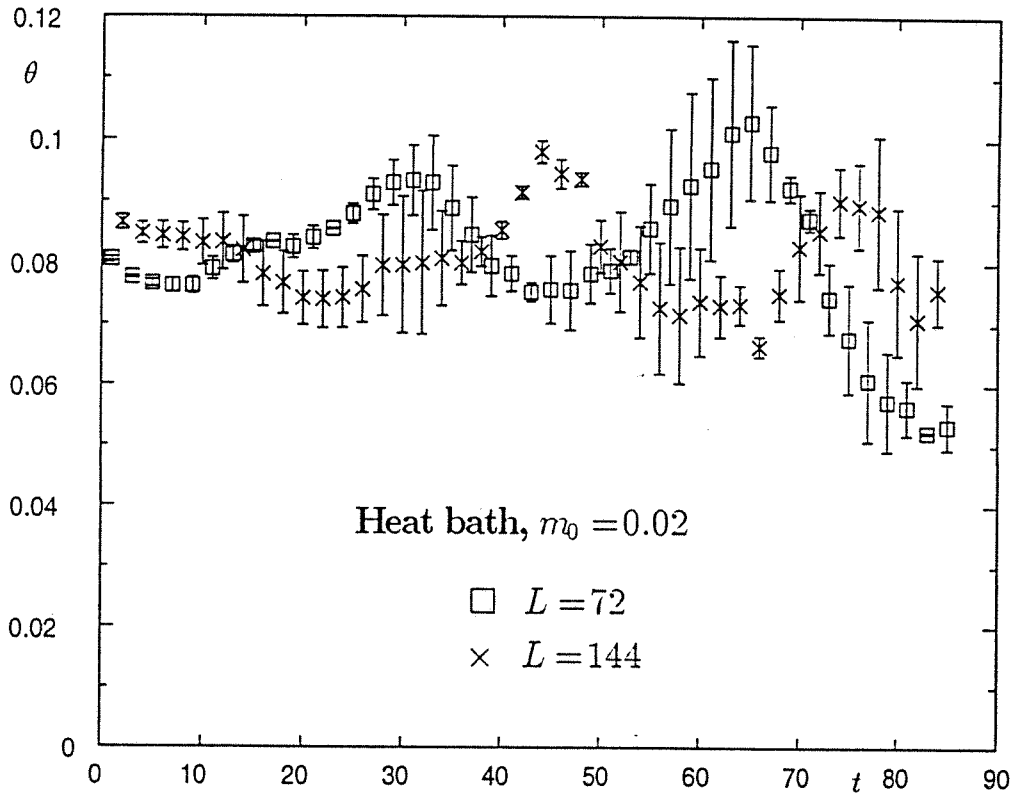

Fig. 6. θ vs. t for the Potts model with $m_0 = 0.02$ and $L = 72, 144$ for the heat-bath algorithm.

beginning. However, for reasons of comparison we treat both algorithms in the same way.

In order to see the finite size effect, we have plotted in Fig. 6 the results of lattices $L = 72$ and $L = 144$ with initial magnetization $m_0 = 0.02$ for the heat-bath algorithm. Within the errors they are overlapping. Therefore we are satisfied with the lattice size $L = 72$ for the measurement of θ. In Table 3 the averaged values of θ for both algorithms still show some slight difference even though for smaller m_0 it looks as if it can be covered by the errors. Similar to the case of the Ising model this may be the remnant of the finite size or finite m_0 effects, or other systematic errors.

From $m_0 = 0.08$ down to $m_0 = 0.02$ the measured θ shows also a smooth linear decrease. Therefore we carry out a linear extrapolation for θ to the initial magnetization $m_0 = 0$. Since here we have measured θ in a different time regime, the result given

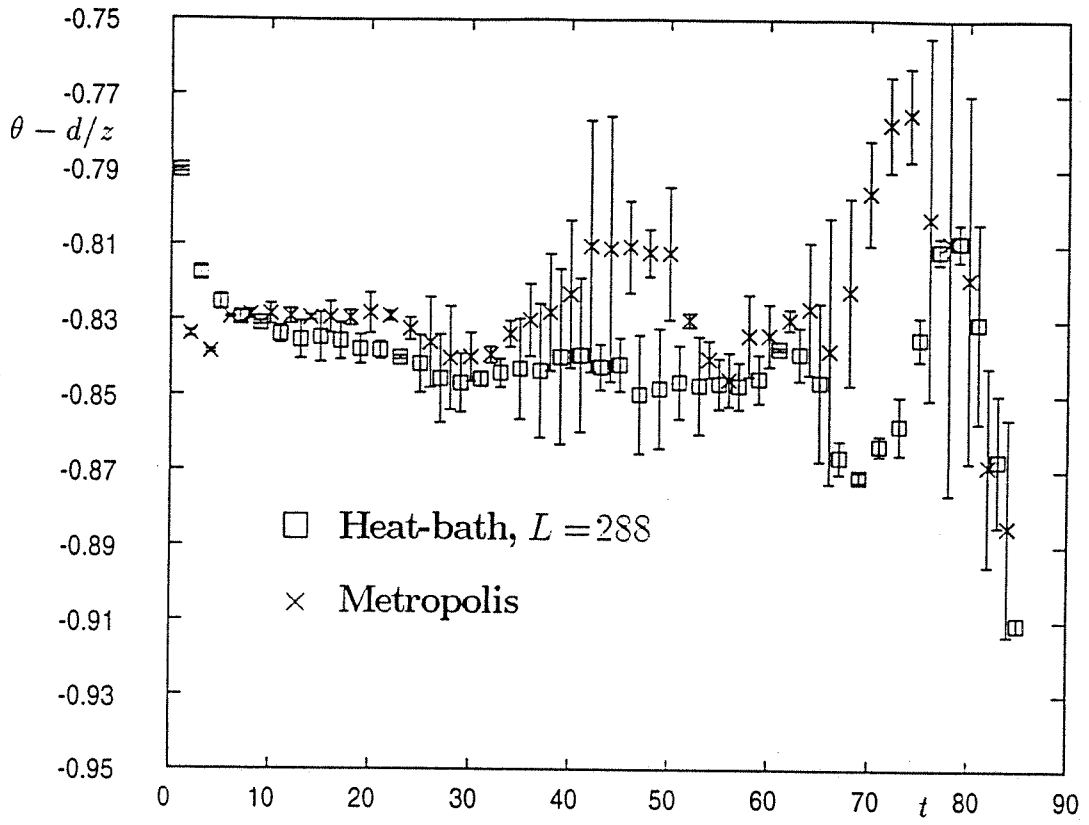

Fig. 7. $\theta - d/z$ vs. t for the Potts model.

in the previous paper [5] for θ has slightly been modified. Due to the extra data for $m_0 = 0.02$ the result extrapolated to $m_0 = 0.0$ is more reliable.

Finally we would like to point out that for the Ising model, the measured θ deceases when m_0 increases, however, for the Potts model it is opposite. This shows that the non-linear (or off-fixed point) correction for the exponent θ when m_0 deviates from the fixed point $m_0 = 0$ are in different directions for these two models [23].

4.2. Auto-correlation

The auto-correlation for the Potts model is given by

$$A(t) = \frac{1}{N}\left\langle \sum_i \left(\delta_{\sigma_i(0),\sigma_i(t)} - \frac{1}{3} \right) \right\rangle . \tag{14}$$

It is known that the dependence of the auto-correlation on the lattice size is bigger than that of the magnetization. Detailed analyses show that we need at least $L = 144$ to observe a clear convergence to the power law decay [5]. This size is bigger than that needed for the magnetization, $L = 72$, by which a nice power law increase has already been observed for the Potts model [5].

In Fig. 7 we present the exponent $\theta - d/z$ obtained by the 15-scan for $L = 288$ as a function of time t for both the heat-bath and the Metropolis algorithm. We ob-

Table 4
The exponent $d/z - \theta$ measured for different lattice sizes with initial magnetization $m_0 = 0.0$ for the Potts model. The last column gives the values for z

L	144	288	576	∞	z
HeatB	0.839(1)	0.834(1)	0.835(1)	0.836(2)	2.196(08)
MetroP	0.849(3)	0.831(2)	0.843(6)	0.841(5)	2.198(13)

serve that the microscopic time scale is quite small, $t_{\mathrm{mic}} \sim 5$. This is also consistent with the tendency discussed in the last section, that the smaller the initial magnetization m_0 is, the shorter the microscopic time scale t_{mic} becomes. For $t > t_{\mathrm{mic}}$ the data obtained from both algorithms well coincide and indicate a quite stable power law behaviour of $A(t)$ in Eq. (7), although the fluctuations for $t \geqslant 50$ become very big. Within the errors both algorithms give almost the same results. However, we should point out that the error for Metropolis is much bigger than that for the heat-bath algorithm. All this shows that for the study of short-time dynamics the heat-bath algorithm is more efficient. In Table 4 the exponent $d/z - \theta$ measured from the time interval [5,50] is listed. To avoid too big fluctuations we have only measured up to $t = 50$. In the previous paper [5], from lattice size $L = 144$ and $L = 288$ a linear extrapolation to infinite lattice size was carried out. However, the result for lattice size $L = 576$ does not go in this direction. Actually the difference between the results for lattices $L = 144, 288, 576$ is already very small as was also pointed out in the previous paper. Therefore in this paper the result for infinite lattice is given as a simple average over the three lattices. The situation for the Metropolis algorithm is less satisfactory. Anyway we also give the same average over the three lattices. From these values as well as those for θ in the previous subsection we can obtain the exponent z.

One can now realize what was mentioned in Section 2. A quite rigorous value for z can be obtained from the measurement of the auto-correlation *if* the exponent θ is known.

In the literature there are several numerical measurements of z [15–18], which predict values for z being distributed between $z = 2.2$ and $z = 2.7$. Our result is supporting a relatively smaller z [15,16]. The results for both algorithms coincide very well. Compared with the results for the Ising model, it seems that the fluctuations in the numerical simulation for the Potts model are smaller.

4.3. The second moment

The second moment for the Potts model is defined by

$$M^{(2)}(t) = \frac{9}{4N^2q} \sum_{r=1}^{q} \left\langle \left[\sum_i \left(\delta_{\sigma_i(t),r} - \frac{1}{3} \right) \right]^2 \right\rangle . \tag{15}$$

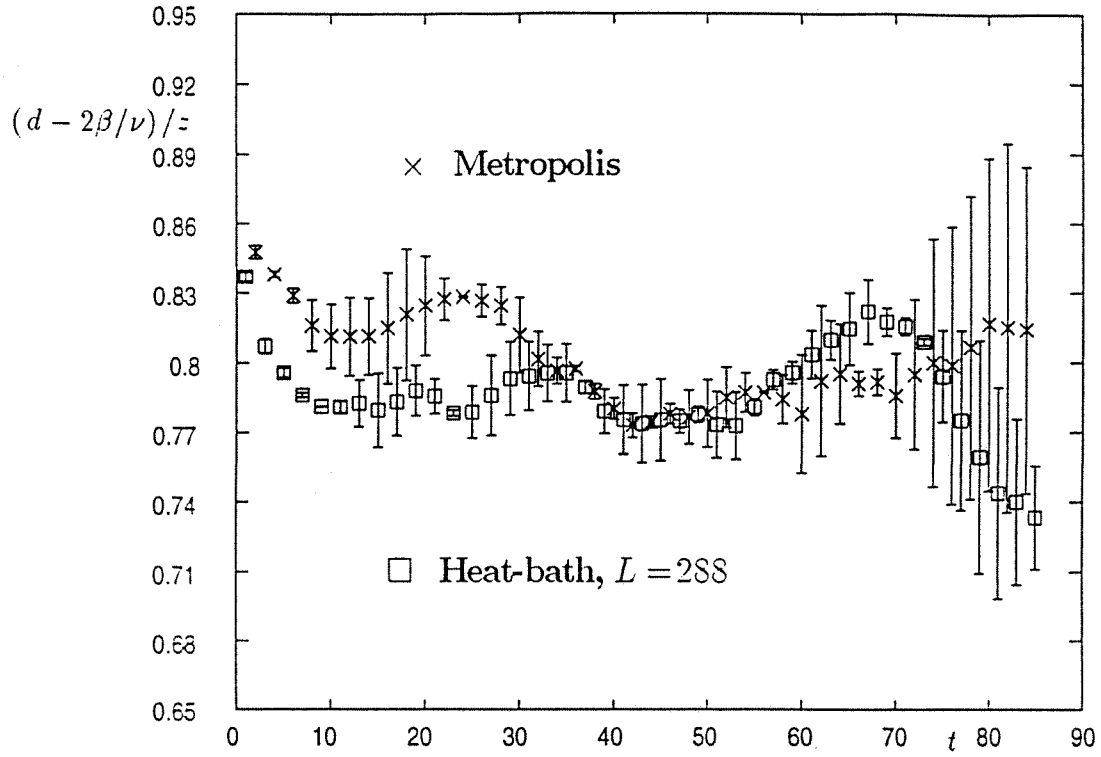

Fig. 8. $(d-2\beta/\nu)/z$ vs. t for the Potts model.

Here we have taken the average over q different components of the variable $\sigma_i(t)$.[2]

We plot the exponent $(d-2\beta/\nu)/z$ for each time step t in Fig. 8. Again it can be realized that the microscopic time scale for heat-bath is smaller than that for Metropolis. However, the exponents for both algorithms coincide after $t_{\text{mic}} \sim 30$. In Table 5 the measured values for $(d-2\beta/\nu)/z$ are given. For the heat-bath algorithm one may start the measurement from $t \sim 10$. However, for the reason of comparison we perform the measurements for both algorithms within a same time interval $[35, 100]$. The results for the lattice $L = 576$ are a bit fluctuating and not given in Table 5. Since the finite size effect is already smaller than the statistical fluctuation, the value of $(d-2\beta/\nu)/z$ for infinite lattice is given as a simple average over $L = 144, 288$.

5. Conclusions and further remarks

We have numerically simulated the short-time critical dynamics for the Ising model and Potts model with special attention to universality. We systematically performed all the simulations with both the heat-bath and Metropolis algorithm in order to investigate universality. By the comparison of those results, we observed that the microscopic time

[2] In the simulation of the magnetization $M(t)$ in Section 4.1, we could also have taken the similar average, in principle. However, we did not do so since the quality of the power law behaviour for different components is not exactly the same.

Table 5
The exponent $(d - 2\beta/\nu)/z$ measured for different lattice sizes with initial magnetization $m_0 = 0.0$ for the Potts model. The last column gives the values for the exponent $2\beta/\nu$

L	144	288	∞	$2\beta/\nu$
HeatB	0.789(2)	0.787(2)	0.788(1)	0.269(07)
MetroP	0.787(7)	0.789(9)	0.788(6)	0.269(16)

scale t_{mic} is not always negligibly small. Universal behaviour appears only after $t > t_{\text{mic}}$. Taking carefully the effect of t_{mic} into account, we obtained reliable critical exponents from the power law behaviour of the observables in the beginning of the time evolution.

For the two-dimensional Potts model, two of us (L.S. and B.Z.) have already reported preliminary results in a previous letter [5], exclusively using the heat-bath algorithm. We have completed the simulations and refined the values of the various exponents, taking seriously the effect of t_{mic} into account. Among the distributed values of the dynamic exponent z for the Potts model [15–18], our result confidently supports relatively smaller ones [15,16].

Traditionally the exponent z is defined in the long-time regime of the dynamic process and normally measured from the exponential decay of the auto-correlation or the magnetization of the systems. This measurement is difficult due to critical slowing down. However, we can obtain the exponent θ from the direct measurement of the initial increase of the magnetization, cf. Eq. (4), therefore the exponent z obtained from the scaling behaviour of the auto-correlation in Eq. (7) is quite rigorous. One may also expect that the measurement is to some extent free from critical slowing down, since all of these quantities are measured in the short-time regime of the dynamic process.

Here we should mention that not all the models will have a positive θ. For example, for the Potts model with $q = 4$ the exponent θ is likely negative or very close to zero. In this case the measurement of θ will become more difficult. On the other hand, how to determine the exponent ν as well as the critical point from the power law behaviour of the observables in the short-time dynamics is also very interesting [8].

Finally we would like to point out that the investigation of the short-time dynamics for statistical systems may be extended to the *dynamic* field theory, e.g. the stochastically quantized field theory where a *fictitious* dynamic process is introduced and the conventional field theory is approached in the equilibrium [24,25]. Detailed investigations have been performed, especially for gauge theory and complex systems [26,27]. However, up to now all these studies are only concentrated to the long-time behaviour of the dynamic process and its equilibrium. It would be very interesting whether the properties of the conventional field theory could also be obtained from the short-time behaviour of the dynamic system. This will be important for the numerical simulation of the lattice gauge theory.

Acknowledgements

L.S. and B.Z would like to thank Z.B. Li for helpful discussions and K. Untch for maintaining the workstations. K.O. is grateful to the DAAD and the JSPS for financial support for his stay in Germany, during which part of the calculations was carried out.

Note added

After the revised version of the paper was completed, we received two preprints from Li and Liu [28] and Ritschel and Czerner [29]. In those papers, some discussions about universality with respect to lattice types and updating schemes are also presented even though the numerical simulation is carried out with relative small lattice sizes where the critical exponent can not confidently be extracted.

References

[1] H.K. Janssen, B. Schaub and B. Schmittmann, Z. Phys. B 73 (1989) 539.
[2] D.A. Huse, Phys. Rev. B 40 (1989) 304.
[3] K. Humayun and A.J. Bray, J. Phys. A 24 (1991) 1915.
[4] Z.B. Li, U. Ritschel and B. Zheng, J. Phys. A: Math. Gen. 27 (1994) L837.
[5] L. Schülke and B. Zheng, Phys. Lett. A 204 (1995) 295.
[6] Z.B. Li, L. Schülke and B. Zheng, Phys. Rev. Lett. 74 (1995) 3396.
[7] Z.B. Li, L. Schülke and B. Zheng, Phys. Rev. E 53 (1996) 2940.
[8] L. Schülke and B. Zheng, Phys. Lett A 215 (1996) 81.
[9] H.K. Janssen, *in* Topics in Modern Statistical Physics, ed. G. Györgyi, I. Kondor, L. Sasvári and T. Tél (World Scientific, Singapore, 1992).
[10] K. Oerding and H.K. Janssen, J. Phys. A: Math. Gen. 26 (1993) 3369, 5295.
[11] K. Oerding and H.K. Janssen, J. Phys. A: Math. Gen. 27 (1994) 715.
[12] U. Ritschel and P. Czerner, Phys. Rev. Lett. 75 (1995) 3882.
[13] P. Czerner and U. Ritschel, Phys. Rev. E 53 (1996) 3333.
[14] A.J. Bray, Adv. Phys. 43 (1994) 357.
[15] M. Aydin and M.C. Yalabik, J. Phys. A: Math. Gen. 18 (1985) 1741.
[16] S. Tang and D.P. Landau, Phys. Rev. B 36 (1987) 567.
[17] K. Binder, Z. Phys. B 43 (1981) 119.
[18] M. Aydin and M.C. Yalabik, J. Phys. A: Math. Gen. 21 (1988) 769.
[19] H.W. Diehl and U. Ritschel, J. Stat. Phys. 73 (1993) 1.
[20] U. Ritschel and H.W. Diehl, Phys. Rev. E 51 (1995) 5392.
[21] P. Grassberger, Physica A 214 (1995) 547.
[22] N. Menyhárd, J. Phys. A: Math. Gen. 27 (1994) 663.
[23] B. Zheng, Phys. Rev. Lett. 77 (1996) 679.
[24] G. Parisi and Y. Wu, Sci. Sin. 24 (1981) 483.
[25] M. Namiki, Stochastic Quantization (Springer, Berlin, 1992).
[26] K. Okano, L. Schülke and B. Zheng, *in* Stochastic Quantization, ed. M. Namiki and K. Okano (Progress of Theoretical Physics, Supplement No. 111, Kyoto, 1993), pp. 313.
[27] K. Fujimura, K. Okano, L. Schülke, K. Yamagishi and B. Zheng, Nucl. Phys. B 424 (1994) 675.
[28] Z. Li and X. Liu, Zhongshan Univ., preprint.
[29] U. Ritschel and P. Czerner, Univ. of Essen, preprint.